

Novel 1,2,3-Triazole-Containing Quinoline-Benzimidazole Hybrids: Synthesis, Antiproliferative Activity, In Silico ADME Predictions, and Docking

Krstulović, L.; Špoljarić Mišković, K.; Rastija, Vesna; Filipović, N.; Bajić, M.; Glavaš-Obrovac, Lj.

Source / Izvornik: **Molecules**, 2023, 28

Journal article, Published version

Rad u časopisu, Objavljena verzija rada (izdavačev PDF)

<https://doi.org/10.3390/molecules28196950>

Permanent link / Trajna poveznica: <https://um.nsk.hr/um:nbn:hr:151:977919>

Rights / Prava: [In copyright](#) / [Zaštićeno autorskim pravom](#).

Download date / Datum preuzimanja: **2024-11-22**



Sveučilište Josipa Jurja
Strossmayera u Osijeku

**Fakultet
agrobiotehničkih
znanosti Osijek**




Repository / Repozitorij:

[Repository of the Faculty of Agrobiotechnical
Sciences Osijek - Repository of the Faculty of
Agrobiotechnical Sciences Osijek](#)



Article

Novel 1,2,3-Triazole-Containing Quinoline–Benzimidazole Hybrids: Synthesis, Antiproliferative Activity, In Silico ADME Predictions, and Docking

Luka Krstulović^{1,*}, Katarina Mišković Špoljarić², Vesna Rastija³, Nikolina Filipović⁴, Miroslav Bajić¹ and Ljubica Glavaš-Obrovac^{2,*}

- ¹ Department of Chemistry and Biochemistry, Faculty of Veterinary Medicine, University of Zagreb, Heinzelova 55, 10000 Zagreb, Croatia; mbajic@vef.hr
- ² Department of Medicinal Chemistry, Biochemistry and Clinical Chemistry, Faculty of Medicine, Josip Juraj Strossmayer University of Osijek, Josipa Huttlera 4, 31000 Osijek, Croatia; kmiskovic@mefos.hr
- ³ Faculty of Agrobiotechnical Sciences Osijek, Josip Juraj Strossmayer University of Osijek, Vladimira Preloga 1, 31000 Osijek, Croatia; vrastija@fazos.hr
- ⁴ Department of Chemistry, Josip Juraj Strossmayer University of Osijek, Cara Hadrijana 8a, 31000 Osijek, Croatia; nfilipovic@kemija.unios.hr
- * Correspondence: lkrstulovic@vef.hr (L.K.); lgobrovac@mefos.hr (L.G.-O.)

Abstract: The newly synthesized quinoline–benzimidazole hybrids containing two types of triazole-methyl-phenoxy linkers were characterized via NMR and elemental analysis. Additional derivatization was achieved by introducing bromine at the C-2 position of the phenoxy core. These novel hybrids were tested for their effects on the growth of the non-tumor cell line MRC-5 (human fetal lung fibroblasts), leukemia and lymphoma cell lines: Hut78, THP-1 and HL-60, and carcinoma cell lines: HeLa and CaCo-2. The results obtained, presented as the concentration that achieves 50% inhibition of cell growth (IC₅₀ value), show that the compounds tested affect tumor cell growth differently depending on the cell line and the dose applied (IC₅₀ ranged from 0.2 to >100 μM). The quinoline–benzimidazole hybrids tested, including 7-chloro-4-(4-[[4-(5-methoxy-1H-1,3-benzodimidazol-2-yl)phenoxy]methyl]-1H-1,2,3-triazol-1-yl)quinoline **9c**, 2-(3-bromo-4-[[1-(7-chloroquinolin-4-yl)-1H-1,2,3-triazol-4-yl]methoxy]phenyl)-N-propyl-1H-benzodimidazol-5-carboximidamide trihydrochloride **10e**, 2-[4-[[1-(2-[(7-chloroquinolin-4-yl)amino]ethyl)-1H-1,2,3-triazol-4-yl]methoxy]phenyl)-N-propyl-1H-benzodimidazol-5-carboximidamide trihydrochloride **14e** and 2-[3-bromo-4-[[1-(2-[(7-chloroquinolin-4-yl)amino]ethyl)-1H-1,2,3-triazol-4-yl]methoxy]phenyl)-N-propyl-1H-benzodimidazol-5-carboximidamide trihydrochloride **15e**, arrested the cell cycle of lymphoma (HuT78) cells. The calculated ADMET properties showed that the synthesized compounds violated at most two of Lipinski's rules, making them potential drug candidates, but mainly for parenteral use due to low gastrointestinal absorption. The quinoline–benzimidazole hybrid **14e**, which was shown to be a potent and selective inhibitor of lymphoma cell line growth, obtained the highest binding energy (−140.44 kcal/mol), by docking to the TAO2 kinase domain (PDB: 2GCD).

Keywords: 1,2,3-triazole-containing quinoline–benzimidazole hybrids; synthesis; antiproliferative effect; in silico ADME; docking



Citation: Krstulović, L.; Mišković Špoljarić, K.; Rastija, V.; Filipović, N.; Bajić, M.; Glavaš-Obrovac, L. Novel 1,2,3-Triazole-Containing Quinoline–Benzimidazole Hybrids: Synthesis, Antiproliferative Activity, In Silico ADME Predictions, and Docking. *Molecules* **2023**, *28*, 6950. <https://doi.org/10.3390/molecules28196950>

Academic Editors: Theodora Venera Apostol, George Mihai Nitulescu and Laura Ileana Socea

Received: 15 September 2023
Revised: 3 October 2023
Accepted: 4 October 2023
Published: 6 October 2023



Copyright: © 2023 by the authors. Licensee MDPI, Basel, Switzerland. This article is an open access article distributed under the terms and conditions of the Creative Commons Attribution (CC BY) license (<https://creativecommons.org/licenses/by/4.0/>).

1. Introduction

Nitrogen-containing heterocycles are ubiquitous in nature and represent the most common scaffold in approved drugs. An analysis of small molecule therapeutics approved by the FDA in the last five years shows that more than half of the approved drugs contain aromatic *N*-heterocycles [1–5]. *N*-heterocycles are also a component of numerous small molecules that have been approved by the FDA for the treatment of cancer in recent years [6].

Cancer is one of the leading causes of death worldwide, with an estimated 10 million deaths in 2020 [7,8]. Despite tremendous efforts, drug resistance is still one of the main reasons for cancer treatment failure [9,10]. One of the latest strategies for cancer therapy is the use of molecular hybrids. The goal of molecular hybridization is the covalent binding of two or more pharmacophores in a single molecule that has the ability to eliminate drug resistance and improve selectivity [11–13]. We aimed to apply this approach to the preparation of hybrids containing quinolines linked to benzimidazoles via a 1,4-disubstituted 1,2,3-triazole linker. To this end, we used a well-known, robust, reliable, and efficient copper-catalyzed cycloaddition of azides and terminal alkynes [14].

Click chemistry has made compounds containing 1,2,3-triazole readily available. Due to its ability to act as a linker, pharmacophore and bioisoster, the 1,2,3-triazole motif is of great importance in drug discovery and can be found in the structures of drug candidates and approved drugs [15–17].

Over the years, numerous triazole compounds have also been tested as potential anticancer drugs [17–20]. Carboxyamidotriazole, shown in Figure 1, is a calcium channel blocker with a 1,4,5-disubstituted 1,2,3-triazole backbone. Recently, carboxyamidotriazole has been clinically investigated as an orotate prodrug salt in non-small cell lung cancer, glioblastoma, and anaplastic glioma [21,22].

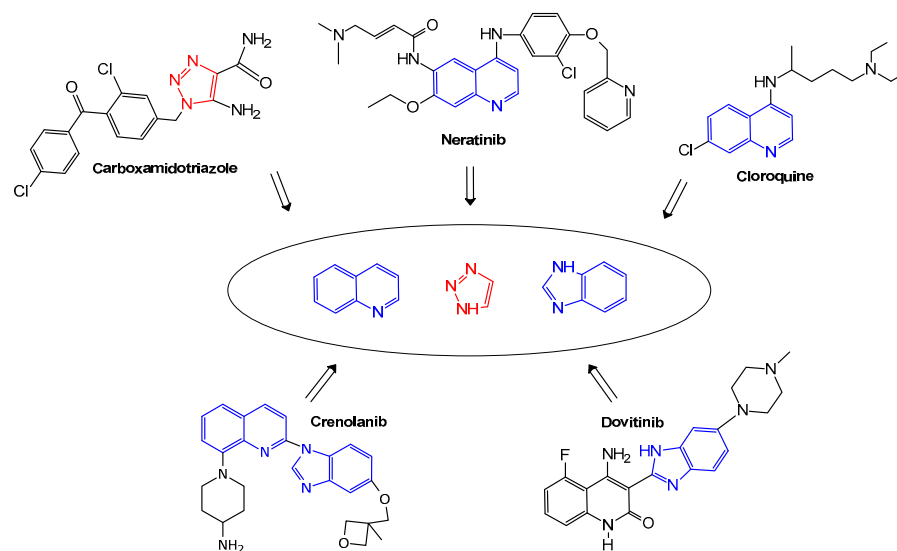


Figure 1. Design of novel triazole-containing benzimidazole–quinoline hybrids.

Quinoline is one of the preferred scaffolds in drug discovery and there are numerous reports on the antiviral, antibacterial, antifungal, antiviral, and antiparasitic activities of compounds with quinoline structure [23,24]. For years, quinoline has played an important role in the discovery of anti-cancer agents [25,26]. The 4-amino-7-chloroquinoline-based antimalarials chloroquine and hydroxychloroquine have been studied in more than sixty clinical trials as anticancer therapies (Figure 1) [27]. Neratinib, shown in Figure 1, is a quinoline-based therapeutic that acts as a tyrosine kinase inhibitor and is used to treat the early and advanced stages of HER-2 positive breast cancer. It has also been clinically evaluated for the treatment of patients with HER-2 mutated advanced bile duct cancer [28–30]. Benzimidazole, also known as 1*H*-benzimidazole and 1,3-benzodiazole, is an aromatic bicyclic *N*-heterocycle containing a benzene ring fused to an imidazole ring. Benzimidazole-containing compounds have shown a wide range of biological activities and have been attracting attention in the drug discovery field for years [31,32]. The benzimidazole backbone is present in several drugs approved for cancer therapy [33]. A patent survey of benzimidazoles shows that more than half of the new benzimidazole compounds were developed for cancer treatment during the indicated period [34]. Crenolanib (Figure 1) is in clinical trials for acute myeloid leukemia and acts as an FMS-like tyrosine kinase-3

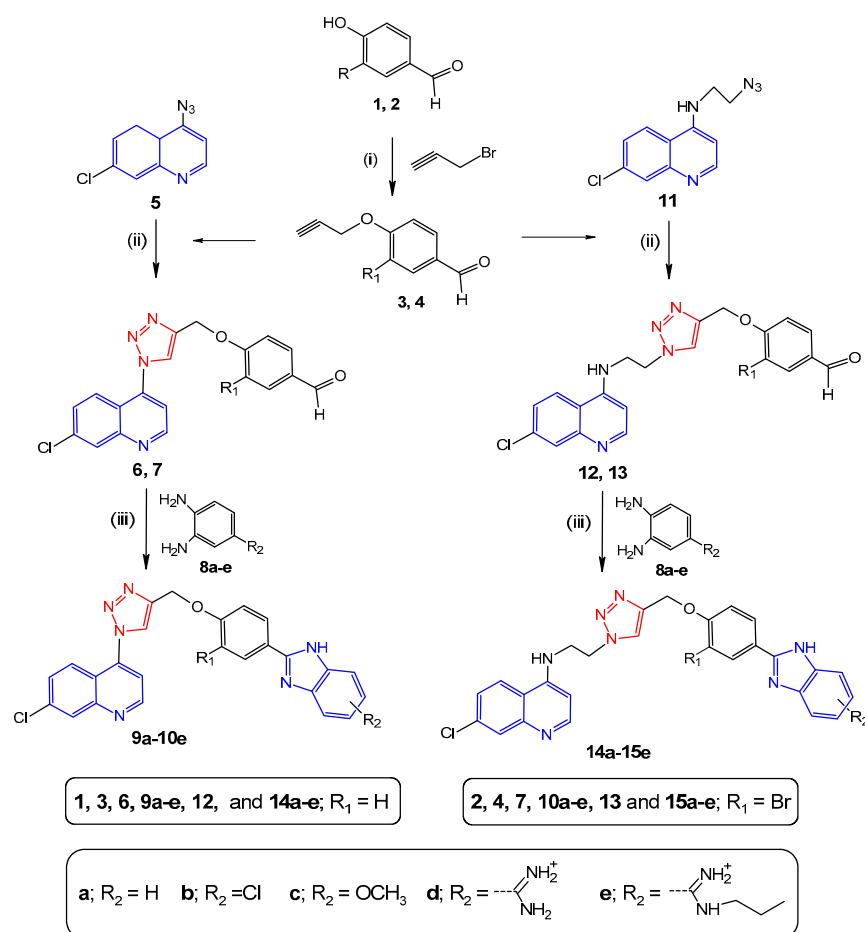
inhibitor. Structurally, it is a compound containing a benzimidazole directly linked to a quinoline moiety [35,36]. Dovitinib is also an anticancer agent containing a benzimidazole scaffold directly linked to a quinolinone. It is a tyrosine kinase inhibitor and has been used in clinical trials to treat patients with advanced pancreatic cancer [37].

Considering the antiproliferative activity of compounds with the above components and continuing our work on quinoline–benzimidazole hybrids [38,39], we report here our next step in the search for anticancer agents, which involves the synthesis of triazole-linked quinoline–benzimidazole hybrids and the evaluation of their antiproliferative activity. To elucidate the possible mechanisms of the antiproliferative activities of the investigated compounds, we performed a molecular docking study on TAO2 (thousand-and-one amino acids) protein kinase. In addition, *in silico* physicochemical and pharmacokinetic/ADMET studies (absorption, distribution, metabolism, excretion, and toxicity) were performed to theoretically predict their behavior as drug candidates.

2. Results and Discussion

2.1. Chemistry

The synthesis of the new quinoline–benzimidazole compounds **9a–10e** and **14a–15d** was carried out as shown in Scheme 1. We prepared hybrid molecules containing quinoline and benzimidazole units linked to two types of triazole methyl phenoxy linkers. The target compounds bear two non-amidine and two amidine substituents at the C-5 position of the benzimidazole molecule. We attempted additional derivatization with a bromine substituent at the C-2 position of the phenoxy core.



Scheme 1. Reagents and reaction conditions: (i) K_2CO_3 , DMF, 30 °C, 24 h; (ii) sodium ascorbate, $CuSO_4$, DMF, 65 °C, 24 h; (iii) $Na_2S_2O_5$, DMSO, 165 °C, 15 min.

The required intermediates **3**, **4**, **5**, and **11** as well as benzene-1,2-diamines **8d–e** were prepared according to the previously reported procedures [40–42].

Triazole intermediates **6**, **7**, **12**, and **13** were synthesized using a partially modified Cu(I)-catalyzed azide-alkyne cycloaddition previously reported by Guntai et al. [40]. Target compounds **9a–10e** and **14b–15d** were prepared using triazole intermediates and the corresponding benzene-1,2-diamines **8a–e** in the presence of sodium metabisulfite in DMSO at 165 °C [43].

2.2. Biological Activity

2.2.1. Evaluation of Antiproliferative Activity of the Novel Compounds

The newly synthesized 1,2,3-triazole-containing quinoline–benzimidazole hybrids were tested to determine their effect on cell growth. The cell lines selected for evaluation included a range of non-tumor and tumor cells: MRC-5 (human fetal lung fibroblasts, non-tumor), Hut78 (T-cell lymphoma), THP-1 (acute monocytic leukemia), HL-60 (acute promyelocytic leukemia), HeLa (human cervical adenocarcinoma), and CaCo-2 (adenocarcinoma of colon). The results of the experiments, quantified according to the concentration at which 50% growth inhibition (IC_{50} value) was achieved, showed different effects of the studied compounds on tumor cell growth. The results depended on factors such as the cell line tested and the dose administered. This suggests that the effects of the compounds on cell growth are influenced by a complex interplay of factors, including their chemical structure, cellular context, and dose-dependent effects.

As shown in Table 1, the IC_{50} values ranged from 0.18 to over 100 μM for all compounds tested. Carcinoma cell lines were more resistant to the tested compounds compared to leukemia and lymphoma cells. In the group of non-amidine compounds without ethylamino linker (**9a–9c**), it was observed that compound **9c** with the methoxy group on the benzimidazole moiety (R_2) exhibited the highest cytotoxicity and showed a non-selective effect against tumor cells compared to normal cells (Figure 2). Although **9c** showed a significant effect on the growth of normal MTR-5 cells with a IC_{50} of 2.71 μM , its selectivity index (SI) was 15 for THP cells (IC_{50} : 0.18 μM) and 13.55 for HuT78 cells (IC_{50} : 0.18 μM). Amidine compounds **9d** and **9e**, containing amidine and propylamide substituents on the benzimidazole core, respectively, caused a selective and pronounced antiproliferative effect on HuT78 cells (**9d**: IC_{50} = 2.52 μM ; SI = 39.7; **9e**: IC_{50} = 10.2 μM ; SI = 9.8).

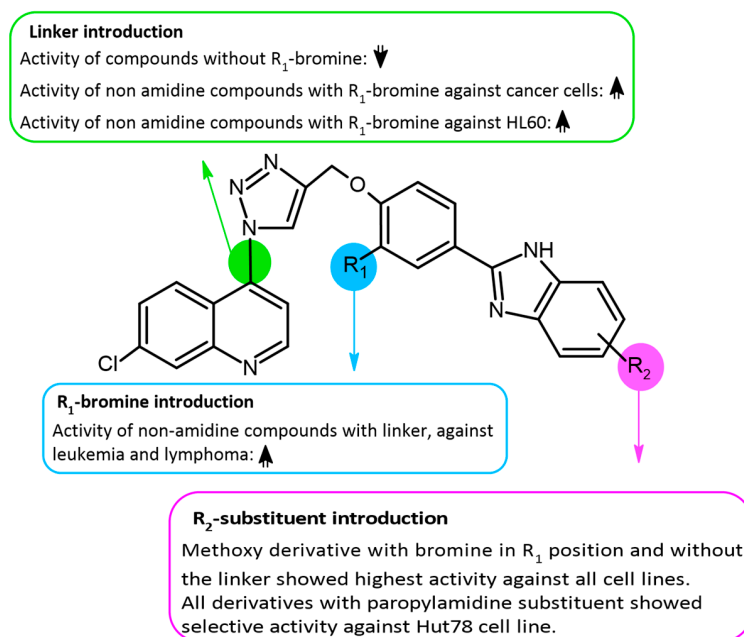
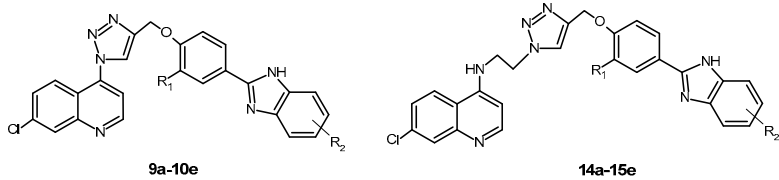
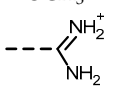
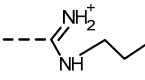
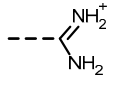
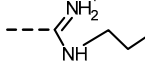
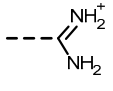
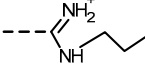
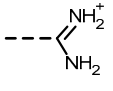
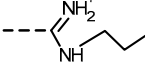


Figure 2. Structure activity relationship for antiproliferative activity of the 1,2,3-triazole-containing quinoline–benzimidazole hybrids.

Table 1. Sensitivity of human tumor and normal cells to investigated compounds expressed as IC₅₀^a value.

Comp.	R ₁	R ₂	MRC-5	HeLa	CaCo-2	THP-1	Hut78	HL-60
								
9a	H	H	>100	>100	>100	>100	100	>100
9b	H	Cl	100	94.1	>100	>100	92.9 ± 4.3	>100
9c	H	OCH ₃	2.71	7.53	8.3	0.18	0.2	1.02
9d	H		>100	>100	>100	>100	2.52	>100
9e	H		>100	>100	>100	>100	10.2	98.3
10a	Br	H	52.1	10.0	63.8	9.6	5.88	76.1
10b	Br	Cl	>100	8.11	10.9	10.6	6.43	55.2
10c	Br	OCH ₃	8.54	9.86	9.92	6.23	3.89	18.2
10d	Br		>100	>100	>100	>100	>100	>100
10e	Br		>100	>100	>100	>100	9.68	93.2
14a	H	H	>100	>100	>100	>100	>100	>100
14b	H	Cl	>100	>100	>100	>100	>100	>100
14c	H	OCH ₃	>100	>100	>100	7.31	>100	>100
14d	H		>100	>100	>100	>100	10.51	>100
14e	H		>100	>100	>100	>100	10.86	>100
15a	Br	H	>100	>100	>100	4.66	7.88	11.63
15b	Br	Cl	>100	>100	>100	2.06	4.91	1.24
15c	Br	OCH ₃	>100	>100	>100	1.65	3.98	2.62
15d	Br		>100	>100	>100	>100	>100	>100
15e	Br		>100	>100	>100	>100	7.83	>100
5-FU			54.1	8.2	5.9	76.4	>100	>100

^a IC₅₀—concentration of the compound that inhibits cell growth by 50%. Data represent mean IC₅₀ (μM) values ± standard deviation (SD) from three independent experiments. Exponentially growing cells were treated with compounds during 72 h. Cytotoxicity was analyzed using MTT survival assay. **5-FU**: 5-fluorouracil.

In the group of compounds without ethylamino linker and with added bromine at the phenoxy core (**10a–e**), the non-amidine compounds **10a** and **10b** showed increased toxicity against both normal and tumor cell lines. The replacement of hydrogen with chlorine at the benzimidazole in **10b** increased antiproliferative activity in all tumor cell lines tested compared with the effect of **9b**. Compound **10c**, which has a methoxy group on the benzimidazole, showed lower cytotoxic activity than compound **9c**, which lacked the bromine substitution at the R₁ position. Compound **10d** (with an amidine group at the R₂

position) showed insignificant inhibitory potential against normal and tumor cells, while derivative **10e** (with a propylamidine group at the R₂ position) showed selective activity against HuT78 cells in terms of growth of normal cells (IC₅₀ = 9.68 μM; SI = 9.8).

In the group of quinoline–benzimidazole hybrids bearing an ethylamino linker (**14a–e**), the non-amidine compounds **14a** and **14c** showed no inhibitory effect on the tested cell lines, except for **14c**, which showed selective activity against THP-1 cells (IC₅₀ = 7.31 μM; SI = 13.7). Interestingly, the hybrids with amidine or propylamidine at the C-5 position of the benzimidazole moiety, **14d** and **14e**, showed no growth inhibition in the tested cell lines and showed almost identical selective antiproliferative activity only in HuT78 cells (**14d**: IC₅₀ = 10.51 μM; SI = 9.51; **9e**: IC₅₀ = 10.86 μM; SI = 9.2).

The introduction of bromine at the phenoxy core in the group of quinoline–benzimidazole hybrids containing an ethylamino linker (**15a–e**) significantly alters the inhibitory effects of non-amidine compounds **15a–c** on the growth of leukemia and lymphoma cells compared to non-substituted non-amidine compounds **14a–c** (Table 1 and Figure 2). Compared with MRC-5 cells and carcinoma cell lines, **15a–c** showed significant antiproliferative activity against lymphoma cells HuT78 (IC₅₀ ranged from 3.98 to 7.88 μM and leukemia cells (HL-60: IC₅₀ ranged from 1.21 to 11.63 μM; THP1: IC₅₀ ranged from 1.65 and 4.66 μM).

No significant difference in the antiproliferative effect was observed between the normal MRC-5 and carcinoma cell lines (HeLa and CaCo2) for compounds **15a–c** (Table 1). The introduction of amidine to benzimidazole (**15d**) resulted in a loss of antiproliferative activity, whereas the introduction of propylamidine to benzimidazole (**15e**) resulted in selective activity against HuT78 cells (IC₅₀ = 7.83 μM; SI = 12.8).

2.2.2. Cell Cycle Perturbation

Inducing cell cycle arrest at specific checkpoints and inducing apoptosis are common strategies in cancer treatment with cytotoxic agents. Numerous studies have shown that quinoline- and benzimidazole-based compounds, as well as their hybrids, significantly affect tumor cell growth [44,45]. To determine whether cell cycle arrest underscores the antiproliferative activity that some compounds exhibit at micromolar and submicromolar concentrations against lymphoma and leukemia cells, we tested the cell cycle distribution of HuT-78 treated with hybrids containing amidine or propylamidine at the C-5 position of the benzimidazole moiety (**10e**, **14e** and **15e**), which showed a selective effect on HuT78 cells growth. The effect on the cell cycle of the non-amidine compound without an ethylamino linker, compound **9c**, which has a methoxy group on the benzimidazole core (R₂) and showed submicromolar IC₅ on leukemia and lymphoma cells (Table 1), were also investigated. As shown in Figure 3, compound **9c** caused a statistically significant enrichment of the S fraction (at 31%, $p < 0.05$) and a significant decrease in the G1 phase (at 66.7%, $p < 0.05$) compared to control cells. No significant changes were observed in the other phases of cell cycle. In contrast to compound **9c**, compound **10e** with introduced bromine at the phenoxy core and with a propylamidine group at the R₂ position (without an ethylamino linker) caused a statistically significant increase in the aggregation of cells in the subG0/G1 phase (more than threefold, $p < 0.05$) with a corresponding decrease in the G1, S and G2/M phases of the cell cycle. In addition, the results of the test of the effects of quinoline–benzimidazole hybrids containing an ethylamino linker showed that the compound with propylamidine at the C-5 position of the benzimidazole moiety, **14e**, and the compound with bromide at the phenoxy core, **15e**, similarly affected the cell cycle by increasing the proportion of cells in subG0/G1 phase (**14e**: by 68%; **15e**: by 36%, $p < 0.05$), resulting in a reduction in the number of cells in G1 and G2/M phases compared to untreated cells, while the changes in other phases of the cell cycle were not statistically significant. These results suggest that the entry of treated cells into a new cell cycle is prevented and are consistent with the results published by Zuo at al. and Zhang at al. [46,47]. The subG0/G1 arrest suggests that the initiation of cell cycle arrest may be responsible for the antiproliferative potential. The subG0/G1 peak indicates DNA fragmentation and suggests that the cells die, most likely through apoptosis. The arrest of the cell cycle in the G2/M phase in cells treated with

various benzimidazole derivatives has also been observed in several recently published studies [45]. These compounds likely affect different phases of the cell cycle, resulting in changes in cell proliferation and growth.

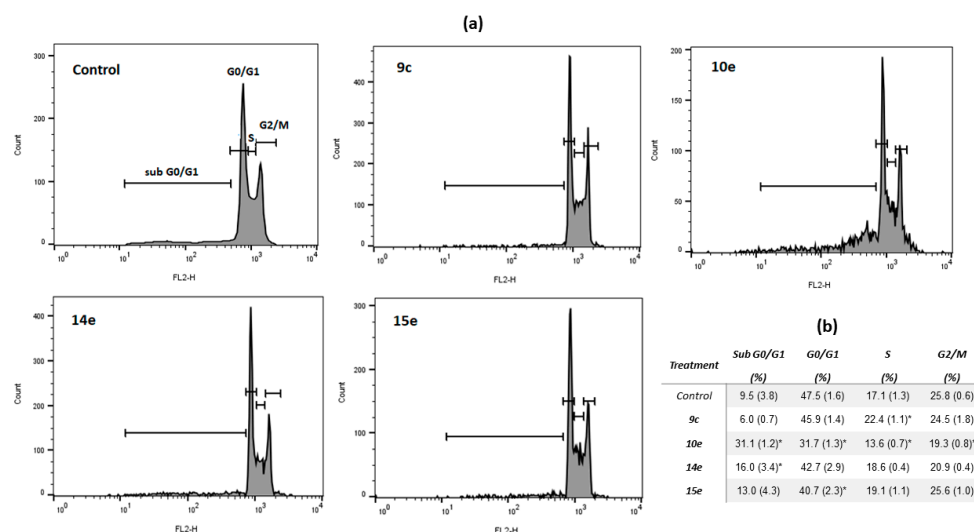


Figure 3. Flow cytometry analysis of the cell cycle distribution of HuT-78 cells exposed to compounds **9c** (0.5 μ M) and **10e**, **14e** and **15e** (5 μ M) for 24 h. (a) DNA histograms present changes in cell cycle. (b) Data are expressed as mean \pm standard deviation. A statistically significant p value is defined as $p < 0.05$ (*).

2.3. Absorption, Distribution, Metabolism, Excretion (ADME), and Toxicity Properties

Calculated ADME, pharmacokinetic and druglike properties of the analyzed compounds were presented in Table 2. According to the “Lipinski’s rule of 5”, the physicochemical ranges for high probability to be an oral drug are molecular weight (MW), between 150 and 500 g/mol; saturation fraction of carbons in the sp^3 hybridization, not less than 0.25; flexibility: rotatable bonds < 9 ; lipophilicity, XLOGP3 between -0.7 and $+5.0$; polarity, topological polar surface area (TPSA) between 20 and 130 \AA^2 ; water solubility, $\log S < 6$ [48].

Table 2. Calculated ADME, pharmacokinetic and druglike properties of the analyzed compounds.

Comp.	MW *	Csp3	RB	HBA	HBD	TPSA	XLOGP3	MLOGP	ESOL Log S	Water Sol.	GIA	BBBP	PgpS	LR
9a	452.9	0.04	5	5	1	81.51	4.97	3.49	-6.12	Poorly	High	No	Yes	0
9b	487.34	0.04	5	5	1	81.51	5.6	3.96	-6.71	Poorly	High	No	Yes	0
9c	482.92	0.08	6	6	1	90.74	4.94	3.17	-6.18	Poorly	High	No	Yes	0
9d	495.94	0.04	6	5	3	133.12	3.94	2.87	-5.62	Poorly	High	No	Yes	0
9e	538.02	0.14	9	5	3	119.13	5.23	3.45	-6.45	Poorly	High	No	Yes	1
10a	531.79	0.04	5	5	1	81.51	5.66	4.32	-7.03	Poorly	High	No	No	2
10b	566.24	0.04	5	5	1	81.51	6.29	4.79	-7.62	Poorly	Low	No	No	2
10c	561.82	0.08	6	6	1	90.74	5.63	3.73	-7.09	Poorly	Low	No	No	1
10d	574.84	0.04	6	5	3	133.12	4.63	3.43	-6.52	Poorly	Low	No	Yes	1
10e	616.92	0.14	9	5	3	119.13	5.92	4.01	-7.36	Poorly	Low	No	No	1
14a	495.96	0.11	8	5	2	93.54	4.93	3.1	-6.11	Poorly	High	No	Yes	0
14b	530.41	0.11	8	5	2	93.54	5.55	3.56	-6.7	Poorly	High	No	No	1
14c	525.99	0.14	9	6	2	102.77	4.9	2.78	-6.18	Poorly	High	No	Yes	1
14d	539.01	0.11	9	5	4	145.15	3.89	2.49	-5.61	Poorly	Low	No	Yes	1
14e	581.09	0.19	12	5	4	131.16	5.19	3.06	-6.45	Poorly	Low	No	No	1
15a	564.86	0.15	9	5	2	93.01	3.74	3.03	-5.52	Moderately	High	No	Yes	1
15b	599.31	0.15	9	5	2	93.01	4.37	3.49	-6.11	Poorly	High	No	No	1
15c	594.89	0.19	10	6	2	102.24	3.72	2.71	-5.6	Moderately	High	No	Yes	1
15d	607.91	0.15	10	5	4	144.62	2.71	2.69	-5.04	Moderately	Low	No	Yes	1
15e	649.99	0.23	13	5	4	130.63	2.71	2.69	-5.04	Moderately	Low	No	Yes	1

* MW (molecular weight, g/mol), Csp³ (fraction of carbons in the sp^3 hybridization); RB (number of rotatable bonds); HBA (number of hydrogen-bond acceptors); HBD (number of hydrogen-bond donors); TPSA (topological polar surface area/ \AA^2); XLOGP3 and MLOGP (lipophilicity descriptors); ESOL Log S (logarithm of the molar solubility in water); Water sol. (water solubility class according the Log S scale); GIA (gastrointestinal absorption); BBBP (blood-brain barrier permeation); PgpS (P-glycoprotein substrate); LR (number of Lipinski rule violations).

The drug similarity of all 20 quinoline–benzimidazole hybrids is schematically represented by the bioavailability radars in the Supplementary Materials (Table S1), while that for the selected molecules is presented in Figure 4.

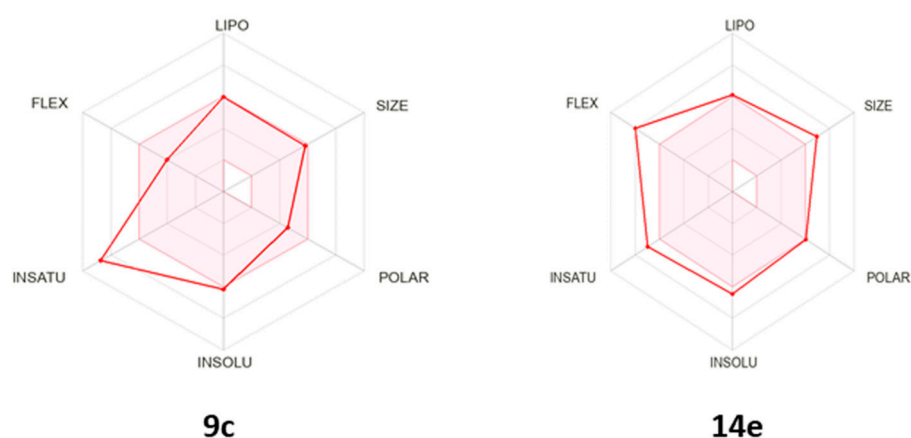


Figure 4. Bioavailability radars for the two most active compounds **9c** and **14e**. The pink area represents the optimal range for each property (lipophilicity (XLOGP3); size (MW); polarity (TPSA); water solubility (log S); saturation (Fraction Csp³); and flexibility (number of rotatable bonds, FLEX).

Six physicochemical properties are taken into account: lipophilicity, size, polarity, solubility, flexibility and saturation [49]. Compound **9c** displayed antiproliferative affinities against all tested tumor cell lines, especially on Hut78 cells (IC₅₀ = 0.2 μM) (Table 1). It also exhibited a toxic effect on normal MTR-5 cells but with great selectivity toward lymphoma cell line Hut78. That compound does not violate either one of the Lipinski rules, making it an ideal drug candidate. According to its bioavailability radar, compound **9c** has optimal range of all properties, except for the fact that it is low in saturation index. It means that the ratio of sp³ hybridized carbons over the total carbon count of the molecule (fraction Csp³) is lower than 0.25. Compound **9c** is poorly soluble in water, but it has high gastrointestinal absorption (GIA), which is important for effective oral drugs. It also has low blood–brain barrier permeation (BBBP), which means that is safe for the unwanted effects of peripheral drugs on the brain (Table 2) [50]. The ability to be transported by P-glycoprotein (P-gp) out of the cell is an important ADME property of compound **9c**. It means that it could be eliminated from cells, thereby preventing intracellular accumulation and decreasing toxicity. Compound **14e** showed strong selective activity against HuT78 cells (IC₅₀ = 10.86 μM) (Table 1). It breaks only one Lipinski rule since it is MW > 500 g/mol (Table 2). The bioavailability radar of compound **14e** reveals its inappropriate drug properties: large size (MW > 500 g/mol); low in saturation index (fraction Csp³ = 0.19); flexibility (number of rotatable bonds > 9). Since that compound is poorly soluble in water, has a low GIA index, and cannot act as a P-glycoprotein substrate, it could only be used for parenteral drug administration.

2.4. Molecular Docking Study

Molecular docking of 20 quinoline–benzimidazole hybrids was performed on the binding site of the TAO2 kinase domain defined according to the bonded ligand staurosporine (STU) (PDB: 2GCD). STU is a well-known inducer of apoptosis in a wide range of the tumor cell lines. The crystal structure of this complex was chosen because it provides the details of the interactions between TAO2 and staurosporine, which explains the relatively low potency of staurosporine against TAO2. Although STU is too toxic to be used directly as a therapeutic agent, it could serve as a template for the design of inhibitors specific to TAO2 [51]. Compounds were ranked by the total energy of the predicted pose in the binding site (Table 3), and the docking scores were compared with the docking results of the staurosporine. The highest binding energy on the TAO2 kinase domain, even before standard ligand staurosporine, was observed for compound **14e** (−140.44 kcal/mol), which has

also exhibited a strong selective antiproliferative effect on HuT78 cells ($IC_{50} = 10.86 \mu M$). The docking result of STU is followed by strong selective inhibitors of HuT78 cells: **9e**, **14d**, **9d**, and **10e**. The energies of the main interactions between compound **14e** and residues in the binding site of the TAO2 kinase are shown in Table 4. The position of this compound into the binding site of the TAO2 kinase domain represented as a hydrophobic surface is shown in Figure 5a, while its interactions with amino acid residues are presented using a 2D diagram (Figure 5b).

Table 3. Total binding energies (kcal/mol) of quinoline–benzimidazole hybrids and standard ligand staurosporine (STU) on TAO2 kinase domain (PDB: 2GCD) with percentage ratio of vdW (van der Waals); (Hbond) hydrogen-bonding; (Elec) electrostatic interactions (%).

Compound	Energy	VDW	HBond	Elec
14e	−140.44	79.20	20.80	0.00
STU	−137.99	89.85	10.15	0.00
9e	−131.00	79.16	20.84	0.00
14d	−127.85	80.96	19.04	0.00
9d	−127.67	72.83	24.98	2.19
10e	−124.68	86.23	13.77	0.00
9c	−123.88	84.30	15.70	0.00
10c	−123.41	78.59	21.41	0.00
9a	−122.31	79.50	20.50	0.00
14a	−120.23	83.55	16.45	0.00
10d	−119.16	81.20	16.97	1.83
10b	−118.41	74.77	25.23	0.00
14c	−116.35	83.43	16.57	0.00
9b	−115.47	85.73	14.27	0.00
15e	−114.44	84.73	15.27	0.00
15c	−111.56	87.59	12.41	0.00
14b	−110.44	81.86	18.14	0.00
10a	−106.61	83.64	16.36	0.00
15a	−105.91	88.73	11.27	0.00
15d	−105.48	88.01	11.99	0.00
15b	−101.95	72.16	27.84	0.00

Table 4. The energies (kcal/mol) of the main interactions between TAO2 kinase domain and compound **14e**.

H Bond	Energy	Van der Waals Interaction	Energy
M-Ile34	−2.30	M-Ile34	−3.95
M-His36	−3.50	M-Gly35	−7.69
S-Glu76	−6.90	M-His36	−7.87
M-Leu80	−1.60	S-His36	−1.21
M-Ile89	−3.50	S-Phe39	−3.82
S-Asp114	−3.50	S-Val42	−3.97
S-Glu117	−5.41	S-Lys57	−6.50
M-Asp169	−2.50	M-Leu80	−3.34
		S-Leu80	−11.43
		M-Ile89	−1.89
		M-Gln90	−7.64
		S-Met105	−8.39
		S-Asp114	−2.81
		S-Glu117	−3.38
		M-Gly168	−4.74
		M-Asp169	−3.88
		S-Asp169	−6.43
		S-Phe170	−3.39
		S-Met312	−2.46
		S-Lys314	−5.48

(M = main chain; S = side chain).

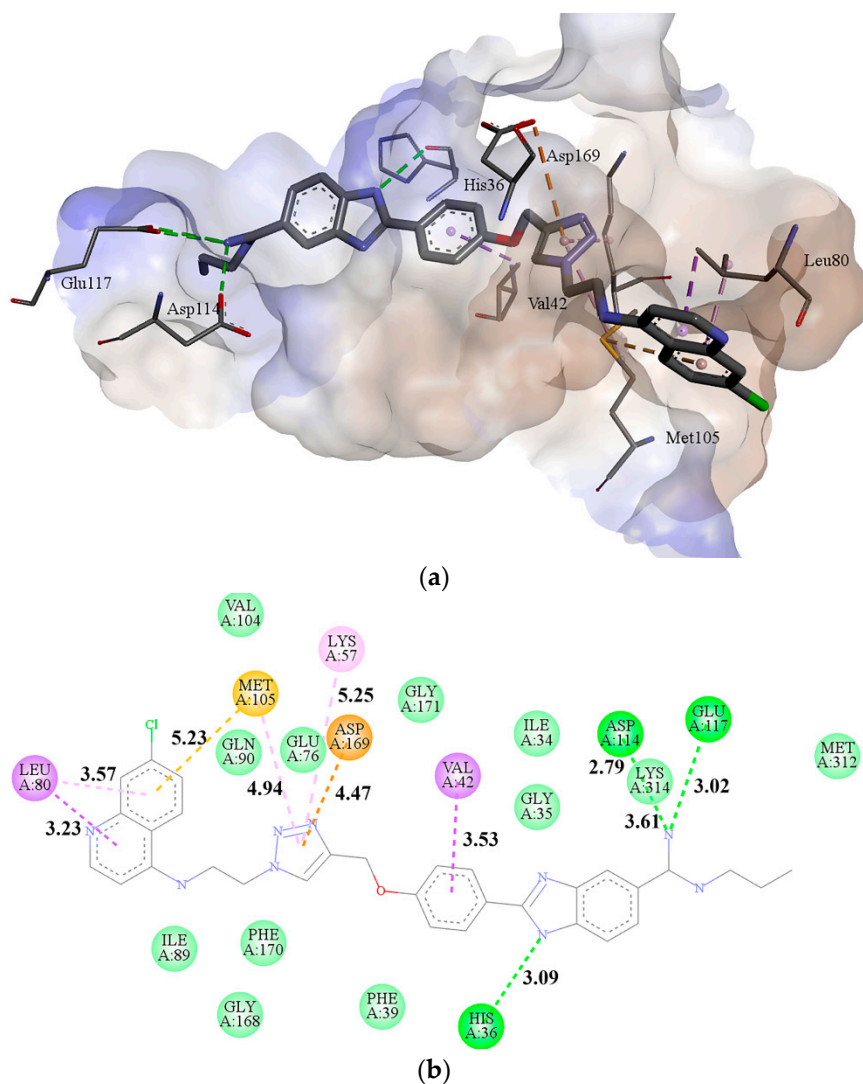


Figure 5. (a) Hydrophobic surface representation of the ATP-binding cleft of TAO2 with docked compound **14e**. (Hydrophobicity range: brown = 3; white = 0; blue = −3); (b) 2D representation of the main interactions between compound **14e** and residues of the TAO2 kinase with the showed distances (Å). (green = conventional hydrogen bond; light green = van der Waals interactions; brown = π -anion; purple = π - σ interactions; pink = π -alkyl interactions).

Compound **14e** is located in the hydrophobic surface of the ATP-binding cleft of the TAO2 due to the presence of plenty of hydrogen bonds and van der Waal interactions. Compound **14e** creates major hydrogen bonds through the N atom of benzimidazole scaffold with His36 (3.09 Å), and the N atom of propilamidine moiety with Asp114 (2.79 Å) and Glu117 (3.02 Å). Van der Waals interactions are very similar to those observed in staurosporine complex with TAO2 kinase (PDB: 2GCD): Gly35; Ile34; Phe39; Glu76; Gln90; Ile89; Gly168; Phe170; Met312. The other interactions are as follows: π - σ interactions (Leu80; Val42); π -anion (Met105; Asp169); π -alkyl interactions (Lys57). We note the very tight π - σ interaction of the quinolone moiety with Leu80 (3.23 Å), leading to a strong interaction energy (11.43 kcal/mol). The interactions between TAO2 and staurosporine involve three hydrogen bonds with Glu106, Cys108, and Gly155 [51].

Mitogen-activated protein kinases (MAPKs) are involved in signal transduction pathways in eukaryotic cells, controlling multiple cellular programs. MAPKs are activated by MAPK kinases. TAO2 is a MAP3K level kinase that activates p38 MAPKs, which regulate the production of cytokines. TAO2 is activated in response to apoptosis-inducing agents

and acts as regulators of apoptosis; it represents a potential drug target for the treatment of cancer [52]. TAO2 is thought to be a physiological regulator of p38 because it is activated during the differentiation of C2C12 myoblasts in parallel with activation of p38 [53]. Therefore, TAO2 is a potential target for the treatment of p38 MAPK-associated diseases such as leukemia, breast cancer, prostate cancer, bladder cancer, liver cancer, lung cancer, thyroid cancer, and many others. Selective inhibitors of TAO2, which inhibit the regulation of MAPK signaling pathway, are used for the development of potential cancer therapy [54].

3. Materials and Methods

3.1. Chemistry

All solvents and reagents were used without purification from commercial sources. To monitor the progress of a reaction and for comparison purposes, thin layer chromatography (TLC) was performed on precoated Merck silica gel 60F-254 plates using an appropriate solvent system, and the spots were detected under UV light (254 nm). Melting points (uncorrected) were determined using the Buchi 510 melting point instrument. ^1H and ^{13}C NMR spectra were recorded using a Bruker Avance DPX-300 or Bruker AV-600 spectrometer. All data were recorded in DMSO- d_6 at 298 K. Chemical shifts were related to the residual solvent signal of DMSO at δ 2.50 ppm for ^1H and δ 39.50 ppm for ^{13}C . Elemental analyses for carbon, hydrogen and nitrogen were performed using the Perkin-Elmer 2400 elemental analyzer. The analyses are given as symbols of the elements. The analytical results obtained are within 0.4% of the theoretical value.

3.1.1. General Procedure for the Synthesis of Compounds 6, 7, 12 and 13

Aldehyde 3 or 4 (1 mmol) and the appropriate azide 5 or 11 (1 mmol) were dissolved in 5 mL DMF and, while stirring at 65 °C, 0.4 mL of 1M sodium ascorbate water solution and 0.2 mL of 1M CuSO_4 water solution were added. The reaction mixture was then stirred at 65 °C for 24 h. The reaction mixture was filtered through a short Al_2O_3 column, with the addition of water, and the product was precipitated.

4-((1-(7-chloroquinolin-4-yl)-1H-1,2,3-triazol-4-yl)methoxy)benzaldehyde (6)

Compound 6 was prepared using the above-described method from 3 (261 mg, 1.5 mmol), 5 (307 mg, 1.5 mmol), 0.6 mL of 1M sodium ascorbate water solution and 0.3 mL of 1M CuSO_4 water solution, as off white product (416 mg, 77%); mp = 188–190 °C. ^1H NMR (600 MHz, DMSO- d_6) δ /ppm 9.91 (s, 1H, CHO), 9.17 (d, J = 4.6 Hz, 1H, ArH), 9.03 (s, 1H, triaz.), 8.30 (d, J = 1.9 Hz, 1H, ArH), 8.00 (d, J = 9.1 Hz, 1H, ArH), 7.92 (d, J = 8.8 Hz, 2H, ArH), 7.89 (d, J = 4.6 Hz, 1H, ArH), 7.80 (dd, J = 2.0 Hz, J = 9.1 Hz, 1H, ArH), 7.33 (d, J = 8.8 Hz, 2H, ArH), 5.47 (s, 2H, CH_2). ^{13}C NMR (151 MHz, DMSO- d_6) δ /ppm 191.33, 162.83, 152.33, 149.34, 142.97, 140.27, 135.37, 131.80, 129.99, 128.97, 127.53, 125.31, 120.26, 117.14, 115.24, 61.20. Anal. calcd. for $\text{C}_{19}\text{H}_{13}\text{ClN}_4\text{O}_2 \times \text{H}_2\text{O}$ (M_r = 382.80): C 59.61, H 3.95, N 14.64; found: C 59.68, H 4.19, N 14.32.

3-bromo-4-[[1-(7-chloroquinolin-4-yl)-1H-1,2,3-triazol-4-yl]methoxy]benzaldehyde (7)

Compound 7 was prepared using the above-described method from 4 (1.08 g, 4.9 mmol), 5 (1 g, 4.9 mmol), 2 mL of 1M sodium ascorbate water solution and 1 mL of 1M CuSO_4 water solution, as an off-white product (1.6 g, 74%); mp = 163–165 °C. ^1H NMR (600 MHz, DMSO- d_6) δ /ppm 9.88 (s, 1H, CHO), 9.17 (d, J = 4.6 Hz, 1H, ArH), 9.03 (s, 1H, triaz.), 8.31 (d, J = 2.1 Hz, 1H, ArH), 8.14 (d, J = 1.9 Hz, 1H, ArH), 7.99 (m, 2H, ArH), 7.90 (d, J = 4.6 Hz, 1H, ArH), 7.81 (dd, J = 2.1 Hz, J = 9.0 Hz, 1H, ArH), 7.65 (d, J = 8.6 Hz, 1H, ArH), 5.58 (s, 2H, CH_2). ^{13}C NMR (151 MHz, DMSO- d_6) δ /ppm 190.54, 158.82, 152.30, 149.34, 142.59, 140.20, 142.59, 135.35, 134.06, 131.05, 130.92, 128.98, 127.26, 125.27, 120.22, 117.14, 114.16, 111.78, 62.32. Anal. calcd. for $\text{C}_{19}\text{H}_{12}\text{ClBrN}_4\text{O}_2 \times 0.5\text{H}_2\text{O}$ (M_r = 452.69): C 50.41, H 2.89, N, 12.38; found: C 50.59, H 2.78, N 12.54.

4-[(1-[2-[(7-chloroquinolin-4-yl)amino]ethyl]-1H-1,2,3-triazol-4-yl)methoxy]benzaldehyde (**12**)

Compound **12** was prepared using the above-described method from **3** (364 mg, 2.1 mmol), **11** (515 mg, 2.1 mmol), 0.84 mL of 1M sodium ascorbate water solution and 0.42 mL of 1M CuSO₄ water solution, as a beige product (648 mg, 76%); mp = 121–123 °C. ¹H NMR (600 MHz, DMSO-*d*₆) δ/ppm 9.87 (s, 1H, CHO), 8.28 (brs+s, 2H, ArH), 7.85 (brs+d, *J* = 8.6 Hz, 3H, ArH), 7.48 (s, 1H, NH), 7.45 (d, *J* = 8.9 Hz, 1H, ArH), 7.20 (d, *J* = 8.6 Hz, 2H, ArH), 6.75 (s, 1H, ArH), 5.25 (s, 2H, CH₂), 4.68 (t, *J* = 5.8 Hz, 2H, CH₂), 3.78 (m, 2H, CH₂). ¹³C NMR (151 MHz, DMSO-*d*₆) δ/ppm 191.26, 162.89, 141.95, 133.18, 131.71, 129.79, 125.31, 124.52, 115.12, 61.41, 47.81, 42.42, 35.79. δ/ppm 190.84. Anal. calcd. for C₂₁H₁₈ClN₅O₂ × 2H₂O (*M*_r = 443.88): C 56.82, H 5.00, N, 15.78; found: C 56.65, H 5.23, N 15.96.

3-bromo-4-[(1-[2-[(7-chloroquinolin-4-yl)amino]ethyl]-1H-1,2,3-triazol-4-yl)methoxy]benzaldehyde (**13**)

Compound **13** was prepared using the above-described method from **4** (400 mg, 1.8 mmol), **11** (442 mg, 1.8 mmol), 0.72 mL of 1M sodium ascorbate water solution and 0.36 mL of 1M CuSO₄ water solution, as a beige product (530 mg, 31%); mp = 125–127 °C. ¹H NMR (600 MHz, DMSO-*d*₆) δ/ppm 9.84 (s, 1H, CHO), 8.75–8.15 (brs+s, 3H, ArH), 8.08 (d, *J* = 1.3 Hz, 1H, ArH), 7.88 (d, 7.48 (s, *J* = 8.5 Hz 1H, ArH), 7.62–7.19 (brs+d+d, *J* = 8.8 Hz, *J* = 8.5 Hz, 4H, NH+ArH), 6.95 (brs, 1H, ArH), 5.36 (s, 2H, CH₂), 4.69 (t, *J* = 5.5 Hz, 2H, CH₂), 3.77 (s, 2H, CH₂). ¹³C NMR (151 MHz, DMSO-*d*₆) δ/ppm 190.49, 158.83, 141.64, 130.95, 130.70, 125.46, 124.85, 124.83, 113.97, 111.64, 62.57, 47.69, 42.54, 35.75. Anal. calcd. for C₂₁H₁₇BrClN₅O₂ × H₂O (*M*_r = 504.76): C 49.97, H 3.79, N, 13.78; found: C 49.74, H 3.98, N 13.95.

3.1.2. General Procedure for the Synthesis of Compounds **9a–10e** and **14a–15e**

A solution of an aldehyde **6**, **12** and **13** (1 mmol) appropriate benzene-1,2-diamine **9a–d** (1 mmol) and Na₂S₂O₅ (0.5 mmol) in DMSO (15 mL) was heated at 165 °C for 15 min. The mixture was cooled down to room temperature. The addition of water (5 mL) resulted in precipitation. The resulting residues for compounds **10a–c**, **11a–c**, **12a–c**, **13a–c**, **14a–c**, **15a–c** were collected with filtration and products were obtained via recrystallization using methanol. The resulting residues for compounds **9d–e**, **10d–e**, **14d–e** and **15d–e** were collected with filtration and products were obtained via recrystallization using methanol and converted to hydrochloride salts using anhydrous methanol saturated with HCl(g).

4-(4-[[4-(1H-benzo[d]imidazol-2-yl)phenoxy]methyl]-1H-1,2,3-triazol-1-yl)-7-chloroquinoline (**9a**)

Compound **9a** was prepared using the above-described method from **6** (300 mg, 0.82 mmol), **8a** (90 mg, 0.82 mmol) and Na₂S₂O₅ (76 mg, 0.41 mmol), as a light brown product (209 mg, 46%); mp = 143–145 °C. ¹H NMR (600 MHz, DMSO-*d*₆) δ/ppm 9.17 (d, *J* = 4.6 Hz, 1H, ArH), 9.05 (s, 1H, triaz.), 8.31 (d, *J* = 1.9 Hz, 1H, ArH), 8.19 (d, *J* = 8.8 Hz, 2H, ArH), 8.02 (d, *J* = 9.1 Hz, 1H, ArH), 7.90 (d, *J* = 4.6 Hz, 1H, ArH), 7.81 (dd, *J* = 2.0 Hz, *J* = 9.1 Hz, 1H, ArH), 7.71 (m, 2H, Ar), 7.46–7.33 (m, 4H, ArH), 5.48 (s, 2H, CH₂). ¹³C NMR (151 MHz, DMSO-*d*₆) δ/ppm 160.52, 152.37, 150.15, 149.36, 143.16, 140.31, 135.39, 129.03, 128.95, 127.14, 125.33, 123.67, 120.29, 119.67, 117.17, 115.60, 114.31, 61.14. Anal. calcd. for C₂₅H₁₇ClN₆O (*M*_r = 452.90): C 66.30, H 3.78, N 18.56; found: C 66.59, H 4.06, N 18.22.

7-chloro-4-(4-[[4-(5-chloro-1H-benzo[d]imidazol-2-yl)phenoxy]methyl]-1H-1,2,3-triazol-1-yl)quinoline (**9b**)

Compound **9b** was prepared using the above-described method from **6** (330 mg, 0.9 mmol), **8b** (129 mg, 0.9 mmol) and Na₂S₂O₅ (85 mg, 0.45 mmol), as a dark brown product (224 mg, 51%); mp = 168–170 °C. ¹H NMR (600 MHz, DMSO-*d*₆) δ/ppm 9.17 (d, *J* = 4.6 Hz, 1H, ArH), 9.03 (s, 1H, triaz.), 8.31 (s, 1H, ArH), 8.16 (d, *J* = 7.9 Hz, 2H, ArH), 8.01 (d, *J* = 9.1 Hz, 1H, ArH), 7.89 (d, *J* = 4.6 Hz, 1H, ArH), 7.81 (dd, *J* = 1.4 Hz, *J* = 9.1 Hz, 1H, ArH), 7.66 (s, 1H, Ar), 7.61 (d, *J* = 8.5 Hz, 1H, ArH), 7.33 (d, *J* = 7.9 Hz, 2H, ArH), 7.26 (d, *J* = 8.5 Hz, 1H, ArH), 5.45 (s, 2H, CH₂). ¹³C NMR (151 MHz, DMSO-*d*₆) δ/ppm 169.80, 152.35, 149.37, 143.29, 140.31, 135.37, 129.02, 128.39, 128.13, 127.07, 125.34, 122.38, 122.05,

120.31, 117.17, 115.87, 115.33, 61.05. Anal. calcd. for $C_{25}H_{16}Cl_2N_6O \times H_2O$ ($Mr = 505.36$): C 59.42, H 3.59, N 16.63; found: C 59.13, H 3.97, N 16.39.

7-chloro-4-(4-[[4-(5-methoxy-1H-benzo[d]imidazol-2-yl)phenoxy]methyl]-1H-1,2,3-triazol-1-yl)quinoline (**9c**)

Compound **9c** was prepared using the above-described method from **6** (300 mg, 0.82 mmol), **8c** (113 mg, 0.82 mmol) and $Na_2S_2O_5$ (76 mg, 0.41 mmol), as a light brown product (190 mg, 49%); mp = 85–86 °C. 1H NMR (600 MHz, DMSO-*d*6) δ /ppm 9.18 (d, $J = 4.6$ Hz, 1H, ArH), 9.04 (s, 1H, triaz.), 8.31 (d, $J = 2.0$ Hz, 1H, ArH), 8.15 (d, $J = 7.2$ Hz, 2H, ArH), 8.01 (d, $J = 9.1$ Hz, 1H, ArH), 7.90 (d, $J = 4.6$ Hz, 1H, ArH), 7.81 (dd, $J = 2.0$ Hz, $J = 9.1$ Hz, 1H, ArH), 7.57 (d, $J = 8.7$ Hz, 1H, ArH), 7.37 (d, $J = 7.7$ Hz, 2H, ArH), 5.46 (s, 2H, CH_2), 3.84 (s, 3H, CH_3). ^{13}C NMR (151 MHz, DMSO-*d*6) δ /ppm 160.17, 156.59, 152.33, 149.40, 143.20, 140.28, 135.37, 129.03, 128.38, 128.16, 127.13, 125.34, 123.67, 120.37, 117.25, 115.55, 112.96, 112.94, 61.11, 55.64. Anal. calcd. for $C_{26}H_{19}ClN_6O_2 \times 0.5H_2O$ ($Mr = 491.93$): C 63.48, H 4.10, N 17.08; found: C 63.75, H 4.37, N 17.21.

2-(4-[[1-(7-chloroquinolin-4-yl)-1H-1,2,3-triazol-4-yl]methoxy]phenyl)-1H-benzo[d]imidazol-5-carboximidamide trihydrochloride (**9d**)

Compound **9d** was prepared using the above-described method from **6** (300 mg, 0.82 mmol), **8d** (123 mg, 0.82 mmol) and $Na_2S_2O_5$ (76 mg, 0.41 mmol), as a brown product (290 mg, 57%); mp = 240–242 °C. 1H NMR (600 MHz, DMSO-*d*6) δ /ppm 9.54 (s, 2H, NH), 9.28 (s, 2H, NH), 9.20 (s, 1H, ArH), 9.09 (s, 1H, triaz.), 8.52 (d, $J = 7.2$ Hz, 2H, ArH), 8.30 (s, 1H, ArH), 8.26 (s, 1H, ArH), 8.03 (d, $J = 9.1$ Hz, 1H, ArH), 7.94 (d, $J = 8.5$ Hz, 1H, ArH), 7.91 (d, $J = 4.5$ Hz, 1H, ArH), 7.87 (dd, $J = 0.9$ Hz, $J = 8.5$ Hz, 1H, ArH), 7.81 (dd, $J = 1.4$ Hz, $J = 9.1$ Hz, 1H, ArH), 7.45 (d, $J = 8.8$ Hz, 2H, ArH), 5.51 (s, 2H, CH_2). ^{13}C NMR (151 MHz, DMSO-*d*6) δ /ppm 165.51, 161.72, 152.20, 149.31, 142.96, 140.32, 135.42, 130.34, 129.08, 128.06, 127.26, 125.38, 124.45, 123.95, 120.39, 117.26, 115.79, 114.78, 114.21, 61.26, 55.64. Anal. calcd. for $C_{26}H_{19}ClN_8O \times H_2O \times 3HCl$ ($Mr = 622.33$): C 50.18, H 3.89, N 18.01; found: C 50.34, H 3.81, N 18.29.

2-(4-[[1-(7-chloroquinolin-4-yl)-1H-1,2,3-triazol-4-yl]methoxy]phenyl)-N-propyl-1H-benzo[d]imidazol-5-carboximidamide trihydrochloride (**9e**)

Compound **9e** was prepared using the above-described method from **6** (300 mg, 0.82 mmol), **8e** (157 mg, 0.82 mmol) and $Na_2S_2O_5$ (76 mg, 0.41 mmol), as a brown product (267 mg, 48%); mp = 228–230 °C. 1H NMR (600 MHz, DMSO-*d*6) δ /ppm 9.99 (t, $J = 4.1$ Hz, 1H, NH), 9.64 (s, 1H, NH), 9.18 (d, $J = 4.6$ Hz, 1H, ArH), 9.17 (s, 1H, NH), 9.09 (s, 1H, triaz.), 8.54 (d, $J = 8.7$ Hz, 2H, ArH), 8.32 (d, $J = 2.1$ Hz, 1H, ArH), 8.18 (d, $J = 1.1$ Hz, 1H, ArH), 8.03 (d, $J = 9.1$ Hz, 1H, ArH), 7.95 (d, $J = 8.5$ Hz, 1H, ArH), 7.91 (d, $J = 4.6$ Hz, 1H, ArH), 7.83 (dd, $J = 2.1$ Hz, $J = 9.1$ Hz, 1H, ArH), 7.79 (dd, $J = 1.1$ Hz, $J = 8.5$ Hz, 1H, ArH), 7.47 (d, $J = 9.0$ Hz, 2H, ArH), 5.52 (s, 2H, CH_2), 3.43 (m, 2H, CH_2), 1.71 (m, 2H, CH_2), 0.99 (t, $J = 7.2$ Hz, 1H, CH_3). ^{13}C NMR (151 MHz, DMSO-*d*6) δ /ppm 162.74, 161.75, 152.31, 151.69, 149.26, 142.96, 140.37, 135.44, 130.34, 129.10, 128.06, 127.27, 125.37, 125.07, 124.62, 123.95, 120.31, 117.20, 115.82, 114.67, 114.18, 114.21, 61.25, 44.38, 20.76, 11.19. Anal. calcd. for $C_{29}H_{25}ClN_8O \times 1.5H_2O \times 3HCl$ ($Mr = 673.42$): C 51.72, H 4.64, N 16.64; found: C 51.40, H 4.89, N 16.26.

4-(4-[[4-(1H-benzo[d]imidazol-2-yl)-2-bromophenoxy]methyl]-1H-1,2,3-triazol-1-yl)-7-chloroquinoline (**10a**)

Compound **10a** was prepared using the above-described method from **7** (300 mg, 0.68 mmol), **8a** (74 mg, 0.68 mmol) and $Na_2S_2O_5$ (65 mg, 0.34 mmol), as a light brown product (167 mg, 47%); mp = 252–254 °C. 1H NMR (600 MHz, DMSO-*d*6) δ /ppm 12.91 (s, 1H, NH), 9.18 (d, $J = 4.5$ Hz, 1H, ArH), 9.04 (s, 1H, triaz.), 8.44 (s, 1H, ArH), 8.31 (d, $J = 2.1$ Hz, 1H, ArH), 8.22 (d, $J = 8.2$ Hz, 1H, ArH), 8.01 (d, $J = 9.1$ Hz, 1H, ArH), 7.91 (d, $J = 4.6$ Hz, 1H, ArH), 7.81 (dd, $J = 2.1$ Hz, $J = 9.1$ Hz, 1H, ArH), 7.65 (d, $J = 8.5$ Hz, 1H, ArH), 7.63 (d, $J = 8.5$ Hz, 1H, ArH), 7.53 (s, 1H, Ar), 7.21 (s, 2H, Ar), 5.55 (s, 2H, CH_2). ^{13}C NMR (151 MHz, DMSO-*d*6) δ /ppm 155.39, 152.35, 149.37, 143.72, 142.96, 140.27, 135.37, 130.91,

129.03, 128.15, 127.19, 127.17, 125.32, 124.64, 122.49, 121.69, 120.32, 118.71, 117.22, 114.66, 111.60, 111.24, 62.15. Anal. calcd. for $C_{25}H_{16}ClBrN_6O \times H_2O$ ($Mr = 549.81$): C 54.61, H 3.30, N 15.29; found: C 54.98, H 3.09, N 15.20.

4-(4-([2-bromo-4-(5-chloro-1H-benzo[d]imidazol-2-yl)phenoxy]methyl)-1H-1,2,3-triazol-1-yl)-7-chloroquinoline (**10b**)

Compound **10b** was prepared using the above-described method from **7** (300 mg, 0.68 mmol), **8b** (96 mg, 0.68 mmol) and $Na_2S_2O_5$ (65 mg, 0.34 mmol), as a brown product (218 mg, 54%); mp = 250–252 °C. 1H NMR (600 MHz, DMSO-*d*₆) δ /ppm 9.18 (d, $J = 4.5$ Hz, 1H, ArH), 9.04 (s, 1H, triaz.), 8.42 (d, $J = 1.5$ Hz, 1H, ArH), 8.30 (d, $J = 2.1$ Hz, 1H, ArH), 8.21 (dd, $J = 1.4$ Hz, $J = 8.6$ Hz, 1H), 8.01 (d, $J = 9.1$ Hz, 1H, ArH), 7.91 (d, $J = 4.6$ Hz, 1H, ArH), 7.81 (dd, $J = 2.1$ Hz, $J = 9.1$ Hz, 1H), 7.64 (d, $J = 8.7$ Hz, 2H, ArH), 7.60 (d, $J = 8.5$ Hz, 1H, ArH), 7.23 (dd, $J = 2.1$ Hz, $J = 8.5$ Hz, 1H), 5.55 (s, 2H, CH₂). ^{13}C NMR (151 MHz, DMSO-*d*₆) δ /ppm 155.71, 152.35, 149.36, 142.91, 140.26, 135.36, 131.10, 129.02, 128.15, 127.43, 127.20, 126.47, 125.31, 123.93, 122.41, 120.29, 117.19, 114.65, 111.63, 111.24, 62.16. Anal. calcd. for $C_{25}H_{16}ClBrN_6O \times 1.5H_2O$ ($Mr = 593.26$): C 50.61, H 3.06, N 14.17; found: C 50.89, H 3.11, N 14.33.

4-(4-([2-bromo-4-(5-methoxy-1H-benzo[d]imidazol-2-yl)phenoxy]methyl)-1H-1,2,3-triazol-1-yl)-7-chloroquinoline (**10c**)

Compound **10c** was prepared using the above-described method from **7** (300 mg, 0.68 mmol), **8c** (92 mg, 0.68 mmol) and $Na_2S_2O_5$ (65 mg, 0.34 mmol), as a light brown product (245 mg, 64%); mp = 170–172 °C. 1H NMR (600 MHz, DMSO-*d*₆) δ /ppm 9.18 (d, $J = 4.6$ Hz, 1H, ArH), 9.05 (s, 1H, triaz.), 8.43 (s, 1H, Ar), 8.31 (d, $J = 2.0$ Hz, 1H, ArH), 8.19 (d, $J = 8.4$ Hz, 1H, ArH), 8.01 (d, $J = 9.1$ Hz, 1H, ArH), 7.91 (d, $J = 4.6$ Hz, 1H, ArH), 7.81 (dd, $J = 2.0$ Hz, $J = 9.1$ Hz, 1H, ArH), 7.69 (d, $J = 8.4$ Hz, 1H, ArH), 7.58 (d, $J = 8.7$ Hz, 1H, ArH), 7.15 (s, 1H, Ar), 6.97 (dd, $J = 1.7$ Hz, $J = 8.4$ Hz, 1H, ArH), 5.57 (s, 2H, CH₂), 3.85 (s, 3H, CH₃). ^{13}C NMR (151 MHz, DMSO-*d*₆) δ /ppm 156.69, 156.11, 152.36, 149.37, 142.82, 140.25, 135.38, 131.22, 129.04, 128.16, 127.59, 127.24, 125.30, 120.29, 117.21, 114.74, 113.14, 111.75, 62.22, 55.64. Anal. calcd. for $C_{26}H_{18}BrClN_6O_2 \times H_2O$ ($Mr = 579.83$): C 53.86, H 3.48, N 14.49; found: C 54.02, H 3.69, N 14.41.

2-(3-bromo-4-([1-(7-chloroquinolin-4-yl)-1H-1,2,3-triazol-4-yl]methoxy)phenyl)-1H-benzo[d]imidazol-5-carboximidamide trihydrochloride (**10d**)

Compound **10d** was prepared using the above-described method from **7** (324 mg, 0.73 mmol), **8d** (109 mg, 0.73 mmol) and $Na_2S_2O_5$ (69 mg, 0.36 mmol), as a dark brown product (263 mg, 63%); mp = 200–202 °C. 1H NMR (600 MHz, DMSO-*d*₆) δ /ppm 9.41 (s, 2H, NH), 9.17 (d, $J = 4.6$ Hz, 1H, ArH), 9.09 (s, 2H, NH), 9.06 (s, 1H, triaz.), 8.59 (d, $J = 2.1$ Hz, 1H, ArH), 8.40 (dd, $J = 2.0$ Hz, $J = 8.6$ Hz, 1H, ArH), 8.30 (d, $J = 2.1$ Hz, 1H, ArH), 8.18 (d, $J = 1.2$ Hz, 1H, ArH), 8.01 (d, $J = 9.1$ Hz, 1H, ArH), 7.91 (d, $J = 4.6$ Hz, 1H, ArH), 7.84 (d, $J = 8.5$ Hz, 1H, ArH), 7.81 (dd, $J = 2.1$ Hz, $J = 9.1$ Hz, 1H, ArH), 7.74 (dd, $J = 1.6$ Hz, $J = 8.5$ Hz, 1H, ArH), 7.70 (d, $J = 8.8$ Hz, 1H, ArH), 5.58 (s, 2H, CH₂). ^{13}C NMR (151 MHz, DMSO-*d*₆) δ /ppm 165.55, 157.53, 152.14, 149.19, 142.65, 140.35, 135.47, 132.67, 129.38, 129.12, 127.97, 127.36, 125.38, 124.30, 123.80, 120.37, 119.05, 117.28, 115.10, 114.73, 114.42, 111.91, 62.32. Anal. calcd. for $C_{26}H_{18}BrClN_8O \times 2H_2O \times 3HCl$ ($Mr = 719.24$): C 43.42, H 3.50, N 15.58; found: C 43.11, H 3.87, N 15.26.

2-(3-bromo-4-([1-(7-chloroquinolin-4-yl)-1H-1,2,3-triazol-4-yl]methoxy)phenyl)-N-propyl-1H-benzo[d]imidazol-5-carboximidamide trihydrochloride (**10e**)

Compound **10e** was prepared using the above-described method from **7** (300 mg, 0.67 mmol), **8e** (128 mg, 0.67 mmol) and $Na_2S_2O_5$ (64 mg, 0.67 mmol), as a dark brown product (214 mg, 52%); mp = 213–214 °C. 1H NMR (600 MHz, DMSO-*d*₆) δ /ppm 9.86 (t, $J = 4.5$ Hz, 1H, NH), 9.53 (s, 1H, NH), 9.18 (d, $J = 4.6$ Hz, 1H, ArH), 9.07 (brs, 2H, NH + triaz.), 8.67 (d, $J = 1.3$ Hz, 1H, ArH), 8.48 (d, $J = 8.5$ Hz, 1H, ArH), 8.32 (d, $J = 2.1$ Hz, 1H, ArH), 8.12 (s, 1H, ArH), 8.02 (d, $J = 9.1$ Hz, 1H, ArH), 7.92 (d, $J = 4.6$ Hz, 1H, ArH), 7.88

(d, $J = 8.5$ Hz, 1H, ArH), 7.83 (dd, $J = 2.1$ Hz, $J = 9.1$ Hz, 1H, ArH), 7.74 (d, $J = 9.1$ Hz, 1H, ArH), 7.70 (dd, $J = 1.1$ Hz, $J = 8.5$ Hz, 1H, ArH), 5.60 (s, 2H, CH₂), 3.42 (m, 2H, CH₂), 1.71 (m, 2H, CH₂), 0.99 (t, $J = 7.1$ Hz, 1H, CH₂). ¹³C NMR (151 MHz, DMSO-*d*₆) δ /ppm 162.70, 157.64, 152.23, 150.56, 149.13, 142.63, 140.39, 135.48, 132.77, 129.50, 129.14, 127.95, 127.38, 125.37, 125.10, 124.61, 120.30, 117.23, 114.91, 114.75, 114.31, 111.94, 62.33, 44.38, 26.15, 20.78, 11.19. Anal. Calcd. For C₂₉H₂₅ClN₈O \times 0.5H₂O \times 3HCl (*M*_r = 734.30): C 47.43, H 3.84, N 15.26; found: C 47.03, H 3.99, N 14.91.

N-[2-(4-[[4-(1H-benzo[d]imidazole-2-yl)phenoxy]methyl]-1H-1,2,3-triazol-1-yl)ethyl]-7-chloroquinolin-4-amine (**14a**)

Compound **14a** was prepared using the above-described method from **12** (300 mg, 0.74 mmol), **8a** (80 mg, 0.74 mmol) and Na₂S₂O₅ (70 mg, 0.37 mmol), as a light brown product (160 mg, 44%); mp = 221–223 °C. ¹H NMR (600 MHz, DMSO-*d*₆) δ /ppm 8.55 (brs, 2H, ArH + triaz.), 8.31 (brs, 2H, ArH), 8.13 (brs, 2H, ArH), 7.63 (brs, 2H, ArH), 7.61 (brs, 2H, ArH + NH), 7.18 (brs, 2H, ArH), 7.16 (brs, 2H, ArH), 6.91 (brs, 1H, ArH), 5.21 (s, 2H, CH₂), 4.72 (s, 2H, CH₂), 3.94 (s, 2H, CH₂). ¹³C NMR (151 MHz, DMSO-*d*₆) δ /ppm 157.29, 142.52, 135.72, 127.83, 126.09, 125.28, 123.08, 121.83, 115.03, 114.84, 61.12, 47.67, 42.77. Anal. calcd. for C₂₇H₂₂ClN₇O \times 0.5H₂O (*M*_r = 504.97): C 64.22, H 4.59, N 19.42; found: C 63.89, H 4.21, N 19.16.

7-chloro-N-[2-(4-[[4-(5-chloro-1H-benzo[d]imidazol-2-yl)phenoxy]methyl]-1H-1,2,3-triazol-1-yl)ethyl]quinolin-4-amine (**14b**)

Compound **14b** was prepared using the above-described method from **12** (300 mg, 0.74 mmol), **8b** (105 mg, 0.74 mmol) and Na₂S₂O₅ (70 mg, 0.37 mmol), as a brown product (160 mg, 44%); mp = 213–215 °C. ¹H NMR (600 MHz, DMSO-*d*₆) δ /ppm 8.43 (s, 1H, ArH), 8.34 (brs, 1H, ArH), 8.31 (s, 1H, ArH), 8.10 (brs, 2H, ArH), 7.89 (brs, 1H, ArH), 7.62 (d, $J = 8.8$ Hz, 2H, ArH), 7.58 (brs, 1H, ArH), 7.19 (d, $J = 8.8$ Hz, 2H, ArH), 7.58 (brs, 1H, ArH), 6.77 (brs, 1H, ArH), 5.21 (s, 2H, CH₂), 4.72 (t, $J = 5.7$ Hz, 2H, CH₂), 3.94 (d, $J = 4.5$ Hz, 2H, CH₂). ¹³C NMR (151 MHz, DMSO-*d*₆) δ /ppm 159.54, 152.67, 147.32, 142.42, 135.85, 128.12, 126.04, 125.80, 125.26, 124.65, 123.39, 122.45, 121.96, 115.08, 115.87, 115.33, 61.16, 55.99, 42.68. Anal. calcd. for C₂₇H₂₁Cl₂N₇O \times H₂O (*M*_r = 548.42): C 59.13, H 4.23, N 17.88; found: C 59.21, H 4.54, N 17.55.

7-chloro-N-[2-(4-[[4-(5-methoxy-1H-benzo[d]imidazol-2-yl)phenoxy]methyl]-1H-1,2,3-triazol-1-yl)ethyl]quinolin-4-amine (**14c**)

Compound **14c** was prepared using the above-described method from **12** (300 mg, 0.74 mmol), **8c** (102 mg, 0.74 mmol) and Na₂S₂O₅ (70 mg, 0.37 mmol), as a brown product (206 mg, 53%); mp = 150–152 °C. ¹H NMR (600 MHz, DMSO-*d*₆) δ /ppm 9.21 (brs, 1H, ArH), 8.52 (brs, 1H, ArH), 8.39 (brs, 1H, ArH), 8.32 (s, 1H, ArH), 8.06 (brs, 2H, ArH), 7.92 (brs, 1H, ArH), 7.75 (d, $J = 8.8$ Hz, 1H, ArH), 7.48 (brs, 1H, ArH), 7.15 (d, $J = 6.7$ Hz, 2H, ArH), 7.09 (brs, 1H, ArH), 6.82 (d, $J = 8.0$ Hz, 2H, ArH), 5.20 (s, 2H, CH₂), 4.75 (t, $J = 5.5$ Hz, 2H, CH₂), 4.05 (s, 2H, CH₂), 3.80 (s, 3H, CH₃). ¹³C NMR (151 MHz, DMSO-*d*₆) δ /ppm 159.17, 155.72, 155.06, 143.90, 142.54, 139.20, 137.72, 127.74, 126.93, 125.33, 125.20, 122.70, 119.97, 115.61, 115.02, 111.38, 61.11, 55.44, 47.77, 42.92. Anal. calcd. for C₂₈H₂₄ClN₇O₂ \times 1.5H₂O (*M*_r = 553.01): C 60.81, H 4.92, N 17.73; found: C 60.43, H 4.99, N 17.40.

2-[4-[(1-[2-[(7-chloroquinolin-4-yl)amino]ethyl]-1H-1,2,3-triazol-4-yl)methoxy]phenyl]-1H-benzo[d]imidazol-5-carboximidamide trihydrochloride (**14d**)

Compound **14d** was prepared using the above-described method from **12** (300 mg, 0.74 mmol), **8d** (111 mg, 0.74 mmol) and Na₂S₂O₅ (70 mg, 0.37 mmol), as a dark brown product (267 mg, 49%); mp = 227–229 °C. ¹H NMR (600 MHz, DMSO-*d*₆) δ /ppm 14.45 (s, 1H, NH), 9.71 (s, 1H, NH), 9.56 (s, 2H, NH), 9.24 (s, 2H, NH), 8.60 (d, $J = 7.2$ Hz, 1H, ArH), 8.47 (brs, 1H, ArH), 8.43 (brs, 1H, ArH), 8.41 (brs, 2H, ArH), 8.05 (brs, 1H, ArH), 7.94 (brs, 1H, ArH), 7.87 (brs, 1H, ArH), 7.74 (d, $J = 7.2$, 1H, ArH), 7.30 (d, $J = 5.6$ Hz, 1H, ArH), 6.76 (brs, 2H, ArH), 5.26 (s, 2H, CH₂), 4.78 (s, 2H, CH₂), 4.07 (s, 2H, CH₂). ¹³C NMR

(151 MHz, DMSO-*d*₆) δ /ppm 165.41, 161.91, 159.17, 155.62, 142.85, 142.03, 138.36, 137.96, 130.40, 126.98, 125.75, 124.79, 124.34, 118.95, 115.72, 115.36, 115.11, 114.63, 114.23, 98.43, 61.44, 47.91, 42.99. Anal. calcd. for C₂₈H₂₄ClN₉O × 2H₂O × 3HCl (Mr = 683.42): C 49.21, H 4.57, N 18.45; found: C 49.56, H 4.70, N 18.17.

2-{4-[(1-[2-(7-chloroquinolin-4-yl)amino]ethyl)-1H-1,2,3-triazol-4-yl]methoxy]phenyl}-N-propyl-1H-benzo[d]imidazol-5-carboximidamide trihydrochloride (**14e**)

Compound **14e** was prepared using the above-described method from **12** (300 mg, 0.74 mmol), **8e** (142 mg, 0.74 mmol) and Na₂S₂O₅ (70 mg, 0.37 mmol), as a dark brown product (210 mg, 49%); mp = 209–211 °C. ¹H NMR (600 MHz, DMSO-*d*₆) δ /ppm 14.31 (s, 1H, NH), 9.88 (s, 1H, NH), 9.62 (t, *J* = 5.1 Hz, 1H, NH), 9.55 (s, 1H, NH), 9.08 (s, 1H, NH), 8.54 (m, 2H, ArH), 8.38 (brs, 2H, ArH), 8.34 (brs, 1H, ArH), 8.13 (brs, 1H, ArH), 8.03 (d, *J* = 1.7, 1H, ArH), 7.91 (d, *J* = 8.5, 1H, ArH), 7.78 (dd, *J* = 1.5 Hz, *J* = 9.1 Hz, 1H, ArH), 7.72 (d, *J* = 8.2, 1H, ArH), 7.29 (d, *J* = 8.2 Hz, 2H, ArH), 6.80 (d, *J* = 7.0 Hz, 2H, ArH), 5.26 (s, 2H, CH₂), 4.79 (t, *J* = 5.1 Hz, 2H, CH₂), 4.08 (m, 2H, CH₂), 3.42 (m, 2H, CH₂), 1.71 (m, 2H, CH₂), 0.94 (t, *J* = 7.3 Hz, 2H, CH₂). ¹³C NMR (151 MHz, DMSO-*d*₆) δ /ppm 162.75, 161.74, 155.64, 142.90, 142.10, 138.36, 138.00, 130.20, 127.01, 125.67, 125.15, 124.66, 119.0, 115.69, 115.36, 114.69, 114.21, 98.45, 61.38, 47.86, 44.38, 42.97, 20.75, 11.21. Anal. calcd. for C₃₁H₃₀ClN₉O × 1.5H₂O × 2HCl (Mr = 716.49): C 51.97, H 5.06, N 17.59; found: C 51.76, H 5.42, N 17.23.

N-[2-(4-[[4-(1H-benzo[d]imidazol-2-yl)-2-bromophenoxy]methyl]-1H-1,2,3-triazol-1-yl)ethyl]-7-chloroquinolin-4-amine (**15a**)

Compound **15a** was prepared using the above-described method from **13** (250 mg, 0.51 mmol), **8a** (55 mg, 0.51 mmol) and Na₂S₂O₅ (50 mg, 0.26 mmol), as a brown product (156 mg, 53%); mp = 155–157 °C. ¹H NMR (600 MHz, DMSO-*d*₆) δ /ppm 8.47 (brs, 1H, ArH), 8.38 (brs, 1H, ArH), 8.31 (s, 1H, ArH), 8.19 (d, *J* = 8.6 Hz, 1H, ArH), 8.14 (dd, *J* = 0.9 Hz, *J* = 8.6 Hz, 1H, ArH), 7.82 (brs, 1H, ArH), 7.63 (brs, 1H, ArH), 7.58 (brs, 2H, ArH), 7.49 (d, *J* = 8.6 Hz, 2H, ArH), 7.19 (m, 2H, ArH), 6.60 (brs, 2H, ArH), 5.32 (s, 2H, CH₂), 4.71 (t, *J* = 5.9 Hz, 2H, CH₂), 3.83 (m, 2H, CH₂), 3.80 (s, 3H, CH₃). ¹³C NMR (151 MHz, DMSO-*d*₆) δ /ppm 155.39, 150.82, 150.00, 141.99, 133.84, 130.81, 127.09, 125.31, 124.64, 124.34, 124.18, 122.06, 115.04, 114.30, 111.41, 62.33, 47.87, 42.42, 40.38. Anal. calcd. for C₂₇H₂₁BrClN₇O × 1.5H₂O (Mr = 601.88): C 53.88, H 4.02, N 16.29; found: C 54.11, H 4.23, N 16.44.

N-[2-(4-[[2-bromo-4-(5-chloro-1H-benzo[d]imidazol-2-yl)phenoxy]methyl]-1H-1,2,3-triazol-1-yl)ethyl]-7-chloroquinolin-4-amine (**15b**)

Compound **15b** was prepared using the above-described method from **13** (300 mg, 0.62 mmol), **8b** (88 mg, 0.62 mmol) and Na₂S₂O₅ (59 mg, 0.31 mmol), as a brown product (195 mg, 50%); mp = 100–102 °C. ¹H NMR (600 MHz, DMSO-*d*₆) δ /ppm 8.36 (brs, 2H, ArH), 8.31 (s, 3H, ArH), 8.12 (d, *J* = 7.9 Hz, 1H, ArH), 7.88 (brs, 1H, ArH), 7.62 (brs, 1H, ArH), 7.60 (d, *J* = 8.8 Hz, 2H, ArH), 7.58 (brs, 1H, ArH), 7.48 (d, *J* = 8.5 Hz, 1H, ArH), 7.22 (dd, *J* = 0.9 Hz, 8.4 Hz, 1H, ArH), 6.74 (brs, 1H, ArH), 5.32 (s, 2H, CH₂), 4.73 (t, *J* = 5.0 Hz, 2H, CH₂), 3.33 (t, *J* = 4.0 Hz, 2H, CH₂). ¹³C NMR (151 MHz, DMSO-*d*₆) δ /ppm 155.60, 150.84, 141.98, 135.34, 130.90, 127.23, 126.33, 125.82, 125.41, 125.09, 123.85, 122.29, 114.27, 111.40, 62.30, 47.79, 42.70. Anal. calcd. for C₂₇H₂₀BrCl₂N₇O × H₂O (Mr = 627.32): C 51.69, H 3.53, N 15.63; found: C 51.76, H 3.90, N 15.27.

N-[2-(4-[[2-bromo-4-(5-methoxy-1H-benzo[d]imidazol-2-yl)phenoxy]methyl]-1H-1,2,3-triazol-1-yl)ethyl]-7-chloroquinolin-4-amine (**15c**)

Compound **15c** was prepared using the above-described method from **13** (266 mg, 0.55 mmol), **8c** (75 mg, 0.55 mmol) and Na₂S₂O₅ (52 mg, 0.31 mmol), as a brown product (186 mg, 55%); mp = 92–94 °C. ¹H NMR (600 MHz, DMSO-*d*₆) δ /ppm 9.24 (s, 1H, ArH), 8.56 (brs, 1H, ArH), 8.41 (d, *J* = 6.0 Hz, 1H, ArH), 8.33 (brs, 1H, ArH), 8.32 (s, 1H, ArH), 8.07 (d, *J* = 7.4 Hz, 1H, ArH), 7.92 (brs, 1H, ArH), 7.77 (d, *J* = 9.0 Hz, 1H, ArH), 7.48 (d, *J* = 8.2 Hz, 2H, ArH), 7.45 (d, *J* = 8.5 Hz, 1H, ArH), 7.07 (s, 1H, ArH), 6.86 (brs, 1H, ArH), 6.83 (dd, *J* = 1.6 Hz, 8.5, 1H, ArH), 5.30 (s, 2H, CH₂), 4.77 (t, *J* = 5.7 Hz, 2H, CH₂), 4.06 (q, *J* = 5.5 Hz,

2H, CH₂), 3.80 (s, 3H, CH₃). ¹³C NMR (151 MHz, DMSO-*d*₆) δ/ppm 155.81, 155.10, 143.63, 142.16, 137.81, 130.49, 127.01, 126.70, 125.47, 125.31, 124.48, 124.46, 114.27, 111.60, 111.34, 62.25, 55.44, 47.79, 42.93. Anal. calcd. for C₂₈H₂₃BrClN₇O₂ × H₂O (Mr = 622.90): C 53.99, H 4.05, N 15.74; found: C 54.26, H 4.41, N 15.41.

2-{3-bromo-4-[(1-[2-[(7-chloroquinolin-4-yl)amino]ethyl]-1H-1,2,3-triazol-4-yl)methoxy]phenyl}-1H-benzo[d]imidazol-5-carboximidamide trihydrochloride (**15d**)

Compound **15d** was prepared using the above-described method from **13** (345 mg, 0.71 mmol), **8d** (106 mg, 0.71 mmol) and Na₂S₂O₅ (67 mg, 0.37 mmol), as a dark brown product (260 mg, 50%); mp = 215–217 °C. ¹H NMR (600 MHz, DMSO-*d*₆) δ/ppm 14.45 (s, 1H, NH), 9.78 (t, *J* = 5.5 Hz, 1H, NH), 9.54 (s, 2H, NH), 9.24 (s, 2H, NH), 8.67 (brs, 2H, ArH), 8.64 (d, *J* = 9.1 Hz, 1H, ArH), 8.52–8.43 (m, 2H, ArH), 8.41 (brs, 1H, ArH), 8.24 (brs, 1H, ArH), 8.08 (d, *J* = 2.0 Hz, 1H, ArH), 7.91 (d, *J* = 8.5 Hz, 1H, ArH), 7.83 (d, *J* = 8.3 Hz, 1H, ArH), 7.75 (dd, *J* = 1.9 Hz, 9.1 Hz, 1H, ArH), 7.57 (d, *J* = 8.5 Hz, 1H, ArH), 6.77 (d, *J* = 7.1 Hz, 1H, ArH), 5.36 (s, 2H, CH₂), 4.82 (t, *J* = 5.5 Hz, 2H, CH₂), 4.36 (s, 2H, CH₂). ¹³C NMR (151 MHz, DMSO-*d*₆) δ/ppm 165.53, 157.41, 155.61, 142.76, 141.79, 138.39, 137.97, 132.53, 129.17, 126.95, 125.80, 124.17, 123.65, 118.94, 115.36, 115.06, 114.42, 111.72, 98.38, 62.49, 47.91, 42.96. Anal. calcd. for C₂₈H₂₃BrClN₉O × 0.5H₂O × 3HCl (Mr = 735.29): C 45.74, H 3.70, N 17.14; found: C 45.41, H 3.94, N 16.92.

2-{3-bromo-4-[(1-[2-[(7-chloroquinolin-4-yl)amino]ethyl]-1H-1,2,3-triazol-4-yl)methoxy]phenyl}-N-propyl-1H-benzo[d]imidazol-5-carboximidamide trihydrochloride (**15e**)

Compound **15e** was prepared using the above-described method from **13** (300 mg, 0.62 mmol), **8e** (119 mg, 0.62 mmol) and Na₂S₂O₅ (59 mg, 0.31 mmol), as a dark brown product (273 mg, 56%); mp = 169–171 °C. ¹H NMR (600 MHz, DMSO-*d*₆) δ/ppm 14.44 (s, 1H, NH), 9.87 (s, 1H, NH), 9.71 (t, *J* = 5.2 Hz, 1H, NH), 9.54 (s, 1H, NH), 9.08 (s, 1H, NH), 8.62 (brs, 1H, ArH), 8.60 (d, *J* = 9.1, 1H, ArH), 8.50 (d, *J* = 6.6, 1H, ArH), 8.40 (brs, 2H, ArH), 8.13 (brs, 1H, ArH), 8.06 (d, *J* = 1.8, 1H, ArH), 7.88 (d, *J* = 7.7, 1H, ArH), 7.76 (dd, *J* = 1.8 Hz, *J* = 9.1 Hz, 1H, ArH), 7.70 (d, *J* = 8.2, 1H, ArH), 7.56 (d, *J* = 8.2 Hz, 1H, ArH), 6.79 (d, *J* = 7.0 Hz, 1H, ArH), 5.36 (s, 2H, CH₂), 4.81 (t, *J* = 5.2 Hz, 2H, CH₂), 4.08 (d, *J* = 5.2 Hz, 2H, CH₂), 3.42 (q, *J* = 6.5 Hz, 2H, CH₂), 1.75–1.66 (m, 2H, CH₂), 0.99 (t, *J* = 7.3 Hz, 2H, CH₂). ¹³C NMR (151 MHz, DMSO-*d*₆) δ/ppm 163.19, 155.67, 143.04, 138.35, 138.10, 128.56, 128.28, 127.09, 127.71, 125.49, 119.10, 114.41, 111.59, 98.53, 62.41, 47.85, 44.29, 42.96, 20.78, 11.20. Anal. calcd. for C₃₁H₂₉BrClN₉O × 0.75H₂O × 3HCl (Mr = 781.87): C 47.62, H 4.32, N 16.12; found: C 47.33, H 3.94, N 15.97

3.2. Biological Activity

3.2.1. Cell Lines and Cell Culturing

The effect of the new synthesized compounds was tested on five human tumor cell lines, HeLa (human cervical adenocarcinoma; from ATCC), CaCo-2 (human colorectal adenocarcinoma), HL-60 (acute promyelocytic leukemia), HuT78 (T-cell lymphoma) and THP-1 (acute monocytic leukemia), and on one non-tumor cell line, MRC-5 (human fetal lung fibroblasts). The MRC-5 cells were used between 24 and 26 passages. The cells were cultured in two different types of media: DMEM (Gibco, EU) and RPMI 1640 (Gibco, EU). Both media were supplemented with 2 mM glutamine, fetal bovine serum (10%; heat inactivated) and antibiotics (100 U penicillin and 0.1 mg streptomycin). RPMI 1640 was additionally supplemented with 10 mM HEPES and 1 mM sodium pyruvate. The cells growing in a monolayer were cultured in DMEM, while the cells growing in suspension were cultured in RPMI 1640. The cells were grown in humidified atmosphere under the conditions of 37 °C/5% CO₂ gas in the CO₂ incubator (IGO 150 CELLlife™, JOUAN, Thermo Fisher Scientific, Waltham, MA, USA).

3.2.2. Proliferation Assay

Growth-inhibitory activity was assessed using a slightly modified procedure based on the National Cancer Institute's protocol [55]. Briefly, the cells were seeded in 96-well microtiter plates and incubated for 24 h. They were then treated with 10^{-7} to 10^{-4} M concentrations of the tested compounds for an additional 72 h. After the treatment period, the effects of the tested compounds on the growth rate of the cells were examined using the MTT assay [56]. Absorbance was measured at 595 nm using a microplate reader. The IC_{50} value, which represents a 50% inhibition of cell growth, and QC calculation were performed using the GraphPadPrism and Excel software. The selectivity index was calculated according to the following formula:

$$SI = \frac{IC_{50} \text{ value of normal cell line}}{IC_{50} \text{ value of cancer cell line}}$$

The effect of each concentration was analyzed by plotting the logarithm of the concentration of the evaluated compound against the corresponding percentage inhibition value using least squares.

3.2.3. Cell Cycle Analysis

HuT78 cells (1×10^5 cells/mL) were seeded in 24-well plates (Falcon, Durham, SAD) and treated with previously determined IC_{50} values for compounds **10e**, **14e**, and **15e** (5×10^{-6} mol/dm³) and **9c** (0.5×10^{-6} mol/dm³). The cells were exposed to the compounds for 24 h, collected, washed with PBS, fixed with 70% ethanol and stored at -20 °C until analysis. On the day of analysis, the cell pellets were washed twice with PBS, resuspended in 1 mg/mL PI and 0.2 mg/mL RNase A and left in a dark/cold atmosphere for 30 min. The stained cells were analyzed using FACSCalibur (Becton Dickinson, Franklin Lakes, NJ, USA) flow cytometer. Tests were performed in duplicate and repeated twice. FlowJo software, version 10.2., was adapted for the analysis of DNA histograms.

STATISTICA 13.5 (TIBCO Software Inc., Tulsa, USA) was used for the statistical analysis of the results. Student's t test was used for data analysis. Differences were considered statistically significant at $p < 0.05$.

3.3. Computational Methods

3.3.1. Calculation of ADME Properties

SwissADME web tool (<http://www.swissadme.ch>, accessed on 25 August 2023) gives free access to a pool of fast yet robust predictive models for physicochemical properties, pharmacokinetics, drug-likeness and medicinal chemistry friendliness parameters through the input of molecular structure [49].

3.3.2. Molecular Docking

Molecular docking of quinoline–benzimidazole hybrids, which exhibited antiproliferative activities, was performed on the MAP3K TAO2 kinase. The crystal structure of the MAP3K TAO2 kinase domain was taken with bounded inhibitor staurosporine from the PDB base (PDB ID: 2GCD). Protein structure was prepared using BIOVIA Discovery Studio Visualizer 4.5 (Dassault Systèmes, Paris, France). The 3D structures of ligands were optimized using Spartan '08 (Wavefunction, Inc.; Irvine, CA, USA, 2009), using the molecular mechanics force field (MM+) [57], and subsequently via the semiempirical AM1 method [58]. The molecular-docking-optimized molecular structures of 12 compounds were performed with iGEMDOCK (BioXGEM, Hsinchu, Taiwan) using generic evolutionary method (GA). The GA parameters were set as follows: population size 200; generations 70; number of poses 3; and binding site radius 8 Å. After each compound was docked into the binding site, iGEMDOCK generated protein–compound interaction profiles of electrostatic (E), hydrogen-bonding (H), and van der Waals (V) interactions. iGEMDOCK infers pharmacological interactions and clusters for post-screening analysis based on these profiles and compound structures. Finally, the docked compounds were ranked by total

energy of a predicted pose in the binding site that is defined as: ($E/\text{kcal mol}^{-1}$) is: $E = \text{vdW} + \text{Hbond} + \text{Elec}$, where the vdW is van der Waal energy, Hbond is the hydrogen bonding energy, and Elec terms are electro statistic energy [59].

4. Conclusions

The targeted 1,2,3-triazole-containing quinoline–benzimidazole hybrids **9a–10e** and **14b–15d** were synthesized via the coupling of phenylenediamines **8a–e** with benzaldehydes **6, 7, 12** and **13** containing 1,4-disubstituted-1,2,3-triazoles prepared via a well-known Cu(I)-catalyzed azide-alkyne cycloaddition reaction.

The results of in vitro studies of antiproliferative activity against one non-tumor and seven cancer cell lines indicate that the introduction of a linker into bromine-substituted non-amidine compounds increases the selectivity and decreases the activity against the carcinoma cell lines tested (HeLa and CaCo2). Chlorine derivatives with bromine and without the linker have selective activity against all cell lines tested. All three non-amidine derivatives with bromine and with a linker showed selective activity against leukemia and lymphoma cells. Non-amidine compounds with a linker showed higher activity against leukemia and lymphoma cells after the introduction of bromine. These compounds affect different phases of the cell cycle, leading to changes in cell proliferation and growth. Cell cycle inhibition may be a key factor in the potential anti-cancer properties of these compounds.

A molecular docking study revealed that the quinoline–benzimidazole hybrid with propylamine at the C-5 position of the benzimidazole moiety, compound **14e**, had the highest affinity to inhibit TAO2 protein kinases, whose activity has been linked to DNA damage and cancer proliferation. This compound showed high and selective antiproliferative activity against lymphoma cell line. Despite its excellent drug-like properties, compound **14e** is not suitable for oral administration due to some deviations in its bioavailability.

Further research and investigation into the mechanisms of action and potential therapeutic applications of these hybrids would be necessary to fully understand their effects on the cell cycle and their ability to induce apoptosis as a mode of treated cell death.

Supplementary Materials: The following supporting information can be downloaded at: <https://www.mdpi.com/article/10.3390/molecules28196950/s1>. Table S1: Bioavailability radars for the 20 quinoline-benzimidazole hybrids. The pink area represents the optimal range for each property (lipophilicity (XLOGP3); size (MW); polarity (TPSA); water sol-ubility (log S); saturation (Fraction Csp3); and flexibility (number of rotatable bonds, FLEX).

Author Contributions: Conceptualization, L.G.-O. and L.K.; synthesis, L.K.; antiproliferative evaluations, K.M.Š., N.F. and L.G.-O.; ADME and molecular docking analysis, V.R.; writing—original draft preparation, L.K., L.G.-O., K.M.Š. and V.R.; writing—review and editing, L.G.-O., L.K., M.B. and V.R.; supervision, L.G.-O., L.K. and V.R.; project administration, L.G.-O.; funding acquisition, L.G.-O. All authors have read and agreed to the published version of the manuscript.

Funding: The biological part of this research was funded by the Faculty of Medicine, Josip Juraj Strossmayer University of Osijek (Institutional project No. IP-08-2022). The synthesis and analysis of the reported compounds was funded by the Faculty of Veterinary Medicine, University of Zagreb (Institutional project No. IP-593-2022).

Institutional Review Board Statement: Not applicable.

Informed Consent Statement: Not applicable.

Data Availability Statement: Not applicable.

Acknowledgments: We greatly appreciate the financial support of the Faculty of Medicine, University of Osijek (project No. IP-08-2022) and the Faculty of Veterinary Medicine, University of Zagreb (Institutional project No. IP-593-2022).

Conflicts of Interest: The authors declare no conflict of interest.

Sample Availability: Samples of the compounds are not available from the authors.

References

1. de la Torre, B.G.; Albericio, F. The Pharmaceutical Industry in 2018. An Analysis of FDA Drug Approvals from the Perspective of Molecules. *Molecules* **2019**, *24*, 809. [[CrossRef](#)] [[PubMed](#)]
2. de la Torre, B.G.; Albericio, F. The Pharmaceutical Industry in 2019. An Analysis of FDA Drug Approvals from the Perspective of Molecules. *Molecules* **2020**, *25*, 745. [[CrossRef](#)]
3. de la Torre, B.G.; Albericio, F. The Pharmaceutical Industry in 2020. An Analysis of FDA Drug Approvals from the Perspective of Molecules. *Molecules* **2021**, *26*, 627. [[CrossRef](#)]
4. de la Torre, B.G.; Albericio, F. The Pharmaceutical Industry in 2021. An Analysis of FDA Drug Approvals from the Perspective of Molecules. *Molecules* **2022**, *27*, 1075. [[CrossRef](#)]
5. de la Torre, B.G.; Albericio, F. The Pharmaceutical Industry in 2022. An Analysis of FDA Drug Approvals from the Perspective of Molecules. *Molecules* **2023**, *28*, 1038. [[CrossRef](#)] [[PubMed](#)]
6. Kumar, A.; Singh, A.K.; Singh, H.; Vijayan, V.; Kumar, D.; Naik, J.; Thareja, S.; Yadav, J.P.; Pathak, P.; Grishina, M.; et al. Nitrogen Containing Heterocycles as Anticancer Agents: A Medicinal Chemistry Perspective. *Pharmaceuticals* **2023**, *16*, 299. [[CrossRef](#)] [[PubMed](#)]
7. Sung, H.; Ferlay, J.; Siegel, R.L.; Laversanne, M.; Soerjomataram, I.; Jemal, A.; Bray, F. Global Cancer Statistics 2020: GLOBOCAN Estimates of Incidence and Mortality Worldwide for 36 Cancers in 185 Countries. *CA Cancer J. Clin.* **2021**, *71*, 209–249. [[CrossRef](#)]
8. Siegel, R.L.; Miller, K.D.; Fuchs, H.E.; Jemal, A. Cancer Statistics, 2022. *CA Cancer J. Clin.* **2022**, *72*, 7–33. [[CrossRef](#)]
9. Nussinov, R.; Tsai, C.J.; Jang, H. Anticancer Drug Resistance: An Update and Perspective. *Drug Resist. Updat.* **2021**, *59*, 100796. [[CrossRef](#)]
10. Emran, T.B.; Shahriar, A.; Mahmud, A.R.; Rahman, T.; Abir, M.H.; Siddiquee, M.F.; Ahmed, H.; Rahman, N.; Nainu, F.; Wahyudin, E.; et al. Multidrug Resistance in Cancer: Understanding Molecular Mechanisms, Immunoprevention and Therapeutic Approaches. *Front. Oncol.* **2022**, *12*, 891652. [[CrossRef](#)]
11. Kumar, S.; Kumar, V. Have molecular hybrids delivered effective anti-cancer treatments and what should future drug discovery focus on? *Expert. Opin. Drug Discov.* **2021**, *16*, 335–363. [[CrossRef](#)]
12. Soltan, O.M.; Shoman, M.E.; Abdel-Aziz, S.A.; Narumi, A.; Konno, H.; Abdel-Aziz, M. Molecular hybrids: A five-year survey on structures of multiple targeted hybrids of protein kinase inhibitors for cancer therapy. *Eur. J. Med. Chem.* **2021**, *225*, 113768. [[CrossRef](#)] [[PubMed](#)]
13. Singh, A.K.; Kumar, A.; Singh, H.; Sonawane, P.; Paliwal, H.; Thareja, S.; Pathak, P.; Grishina, M.; Jaremko, M.; Emwas, A.H.; et al. Concept of Hybrid Drugs and Recent Advancements in Anticancer Hybrids. *Pharmaceuticals* **2022**, *15*, 1071. [[CrossRef](#)]
14. Rostovtsev, V.V.; Green, L.G.; Fokin, V.V.; Sharpless, K.B. A Stepwise Huisgen Cycloaddition Process: Copper(I)-Catalyzed Regioselective “Ligation” of Azides and Terminal Alkynes. *Angew. Chem. Int. Ed.* **2002**, *41*, 2596–2599. [[CrossRef](#)]
15. Jiang, X.; Hao, X.; Jing, L.; Wu, G.; Kang, K.; Liu, X.; Zhan, P. Recent applications of click chemistry in drug discovery. *Expert Opin. Drug Discov.* **2019**, *14*, 779–789. [[CrossRef](#)]
16. Lengerli, D.; Ibis, K.; Nural, Y.; Banoglu, E. The 1,2,3-triazole ‘all-in-one’ ring system in drug discovery: A good bioisostere, a good pharmacophore, a good linker, and a versatile synthetic tool. *Expert Opin. Drug Discov.* **2022**, *17*, 1209–1236. [[CrossRef](#)]
17. Serafini, M.; Pirali, T.; Iron, G.C. Click 1,2,3-triazoles in drug discovery and development: From the flask to the clinic? In *Advances in Heterocyclic Chemistry*; Meanwall, N.A., Lolli, M.L., Eds.; Elsevier Inc.: Amsterdam, The Netherlands, 2021; Volume 134, ISBN 9780128201824. [[CrossRef](#)]
18. Alam, M.M. 1,2,3-Triazole hybrids as anticancer agents. *Arch. Pharm.* **2022**, *355*, 2100158. [[CrossRef](#)] [[PubMed](#)]
19. Liang, T.; Sun, X.; Li, W.; Hou, G.; Gao, F. 1,2,3-Triazole-Containing Compounds as Anti-Lung Cancer Agents: Current Developments, Mechanisms of Action, and Structure–Activity Relationship. *Front. Pharmacol.* **2021**, *12*, 661173. [[CrossRef](#)]
20. Mishra, K.N.; Upadhyay, H.C. Coumarin-1,2,3-triazole hybrids as leading-edge anticancer agents. *Front. Drug. Discov.* **2022**, *2*, 1072448. [[CrossRef](#)]
21. Si, X.; Wang, J.; Cheng, Y.; Shi, J.; Cui, L.; Zhang, H.; Huang, Y.; Liu, W.; Chen, L.; Zhu, J.; et al. A phase III, randomized, double-blind, controlled trial of carboxyamidotriazole plus chemotherapy for the treatment of advanced non-small cell lung cancer. *Ther. Adv. Med. Oncol.* **2020**, *12*, 1–9. [[CrossRef](#)]
22. Omuro, A.; Beal, K.; McNeill, K.; Young, R.J.; Thomas, A.; Lin, X.; Terziev, R.; Kaley, T.J.; De Angelis, L.M.; Daras, M.; et al. Multicenter Phase IB Trial of Carboxyamidotriazole Orotate and Temozolomide for Recurrent and Newly Diagnosed Glioblastoma and Other Anaplastic Gliomas. *J. Clin. Oncol.* **2018**, *36*, 1702–1709. [[CrossRef](#)]
23. Yadav, P.; Shah, K. Quinolines, a perpetual, multipurpose scaffold in medicinal chemistry. *Bioorg. Chem.* **2021**, *109*, 104639. [[CrossRef](#)]
24. Senerovic, L.; Opsenica, D.; Moric, I.; Aleksic, I.; Spasić, M.; Vasiljevic, B. Quinolines and Quinolones as Antibacterial, Antifungal, Anti-virulence, Antiviral and Anti-parasitic Agents. In *Advances in Microbiology, Infectious Diseases and Public Health*; Donelli, G., Ed.; Springer: Cham, Switzerland, 2019; Volume 1282, ISBN 978-3-030-53646-6. [[CrossRef](#)]
25. Basavarajaiah, S.M. The Versatile Quinoline and Its Derivatives as anti-Cancer Agents: An Overview. *Polycycl. Aromat. Compd.* **2022**, *43*, 4333–4345. [[CrossRef](#)]
26. Ilakiyalakshmi, M.; Napoleon, A.A. Review on recent development of quinoline for anticancer activities. *Arab. J. Chem.* **2022**, *15*, 104168. [[CrossRef](#)]

27. Chloroquine and hydroxychloroquine in antitumor therapies based on autophagy-related mechanisms. *Pharmacol. Res.* **2021**, *168*, 105582. [[CrossRef](#)]
28. Holmes, F.A.; Moy, B.; Delalogue, S.; Chia, S.K.L.; Ejlertsen, B.; Mansi, J.; Iwata, H.; Gnant, M.; Buyse, M.; Barrios, C.H.; et al. Overall survival with neratinib after trastuzumab-based adjuvant therapy in HER2-positive breast cancer (ExteNET): A randomised, double-blind, placebo-controlled, phase 3 trial. *Eur. J. Cancer* **2023**, *184*, 48–59. [[CrossRef](#)] [[PubMed](#)]
29. Cunningham, N.; Shepherd, S.; Mohammed, K.; Lee, K.A.; Allen, M.; Johnston, S.; Kipps, E.; McGrath, S.; Noble, J.; Parton, M.; et al. Neratinib in advanced HER2-positive breast cancer: Experience from the royal Marsden hospital. *Breast Cancer Res. Treat.* **2022**, *195*, 333–340. [[CrossRef](#)]
30. Harding, J.J.; Piha-Paul, S.A.; Shah, R.H.; Murphy, J.J.; Cleary, J.M.; Shapiro, G.I.; Quinn, D.I.; Brana, I.; Moreno, V.; Borad, M.; et al. Antitumour activity of neratinib in patients with HER2-mutant advanced biliary tract Cancers. *Nat. Comm.* **2023**, *14*, 630. [[CrossRef](#)]
31. Alzhrani, Z.M.M.; Alam, M.M.; Nazreen, S. Recent Advancements on Benzimidazole: A Versatile Scaffold in Medicinal Chemistry. *Mini Rev. Med. Chem.* **2022**, *22*, 365–386. [[CrossRef](#)] [[PubMed](#)]
32. Ebenezer, O.; Jordaan, M.A.; Carena, G.; Bono, T.; Shapi, M.; Tuszynski, J.A. An Overview of the Biological Evaluation of Selected Nitrogen-Containing Heterocycle Medicinal Chemistry Compounds. *Int. J. Mol. Sci.* **2022**, *23*, 8117. [[CrossRef](#)]
33. Lee, Y.T.; Tan, Y.J.; Oon, C.E. Benzimidazole and its derivatives as cancer therapeutics: The potential role from traditional to precision medicine. *Acta Pharm. Sin. B.* **2022**, *13*, 478–497. [[CrossRef](#)]
34. Law, C.S.W.; Yeong, K.Y. Benzimidazole in Drug Discovery: A patent review. *ChemMedChem* **2021**, *17*, 1861–1877. [[CrossRef](#)]
35. Tarlock, K.; Meshinchi, S.; Rubnitz, J.E.; Karol, S.E.; Spitzer, B.; Sabnitz, A.J.; Pathan, A.; Messahel, B. Clinical Benefit and Tolerability of Crenolanib in Children with Relapsed Acute Myeloid Leukemia Harboring Treatment Resistant FLT3 ITD and Variant FLT3 TKD Mutations Treated on Compassionate Access. *Blood* **2020**, *136*, 23–24. [[CrossRef](#)]
36. Zhang, H.; Savage, S.; Reister Schultz, A.; Bottomly, D.; White, L.; Segerdell, E.; Wilmot, B.; McWeeney, S.K.; Eide, C.A.; Nechiporuk, T.; et al. Clinical resistance to crenolanib in acute myeloid leukemia due to diverse molecular mechanisms. *Nat. Commun.* **2019**, *10*, 244. [[CrossRef](#)] [[PubMed](#)]
37. Ma, W.W.; Xie, H.; Fetterly, G.; Pitzonka, L.; Whitworth, A.; LeVea, C.; Wilton, J.; Mantione, K.; Schihl, S.; Dy, G.K.; et al. A phase Ib study of the FGFR/VEGFR inhibitor dovitinib with gemcitabine and capecitabine in advanced solid tumor and pancreatic cancer patients. *Am. J. Clin. Oncol.* **2019**, *42*, 184–189. [[CrossRef](#)] [[PubMed](#)]
38. Krstulović, L.; Stolić, I.; Jukić, M.; Opačak-Bernardi, T.; Starčević, K.; Bajić, M.; Glavaš-Obrovac, L. New quinoline-arylamidine hybrids: Synthesis, DNA/RNA binding and antitumor activity. *Eur. J. Med. Chem.* **2017**, *137*, 196–210. [[CrossRef](#)] [[PubMed](#)]
39. Krstulović, L.; Leventić, M.; Rastija, V.; Starčević, K.; Jirouš, M.; Janić, I.; Karnaš, M.; Lasić, K.; Bajić, M.; Glavaš-Obrovac, L. Novel 7-Chloro-4-aminoquinoline-benzimidazole Hybrids as Inhibitors of Cancer Cells Growth: Synthesis, Antiproliferative Activity, In Silico ADME Predictions, and Docking. *Molecules* **2023**, *28*, 540. [[CrossRef](#)]
40. Guantai, E.M.; Ncokezi, K.; Egan, T.J.; Gut, J.; Rosenthal, P.J.; Smith, P.J.; Chibale, K. Design, synthesis and in vitro antimalarial evaluation of triazole-linked chalcone and dienone hybrid compounds. *Bioorg. Med. Chem.* **2010**, *18*, 8243–8256. [[CrossRef](#)]
41. Starčević, K.; Pešić, D.; Toplak, A.; Landek, G.; Alihodžić, S.; Herreros, E.; Ferrer, S.; Spaventi, R.; Perić, M. Novel hybrid molecules based on 15-membered azalide as potential antimalarial agents. *Eur. J. Med. Chem.* **2012**, *49*, 365–378. [[CrossRef](#)]
42. Czarny, A.; Wilson, W.D.; Boykin, D.W. Synthesis of mono-cationic and dicationic analogs of Hoechst 33258. *J. Heterocycl. Chem.* **1996**, *33*, 1393–1397. [[CrossRef](#)]
43. Abou-Elkhair, R.A.I.; Hassan, A.E.A.; Boykin, D.W.; Wilson, W.D. Lithium Hexamethyldisilazane Transformation of Transiently Protected 4-Aza/Benzimidazole Nitriles to Amidines and their Dimethyl Sulfoxide Mediated Imidazole Ring Formation. *Org. Lett.* **2016**, *18*, 4714–4717. [[CrossRef](#)] [[PubMed](#)]
44. Diaconu, D.; Antoci, V.; Mangalagiu, V.; Amariuca-Mantu, D.; Mangalagiu, I.I. Quinoline-imidazole/benzimidazole derivatives as dual-/multi-targeting hybrids inhibitors with anticancer and antimicrobial activity. *Sci. Rep.* **2022**, *12*, 1–17. [[CrossRef](#)]
45. Feng, L.; Su, W.; Cheng, J.; Xiao, T.; Li, H.; Chen, D.; Zhang, Z. Benzimidazole Hybrids as Anticancer Drugs: An Updated Review on Anticancer Properties, Structure–Activity Relationship, and Mechanisms of Action (2019–2021). *Arch. Pharm.* **2022**, *355*, 2200051. [[CrossRef](#)]
46. Zuo, D.; Jiang, X.; Han, M.; Shen, J.; Lang, B.; Guan, Q.; Bai, Z.; Han, C.; Li, Z.; Zhang, W.; et al. Methyl 5-[(1H-indol-3-yl)selanyl]-1H-benzimidazol-2-ylcarbamate (M-24), a novel tubulin inhibitor, causes G2/M arrest and cell apoptosis by disrupting tubulin polymerization in human cervical and breast cancer cells. *Toxicol. Vitr.* **2017**, *42*, 139–149. [[CrossRef](#)] [[PubMed](#)]
47. Zhang, L.; Bochkur Dratver, M.; Yazal, T.; Dong, K.; Nguyen, A.; Yu, G.; Dao, A.; Bochkur Dratver, M.; Duhacek-Muggy, S.; Bhat, K.; et al. Mebendazole Potentiates Radiation Therapy in Triple-Negative Breast Cancer. *Int. J. Radiat. Oncol. Biol. Phys.* **2019**, *103*, 195–207. [[CrossRef](#)]
48. Lipinski, C.A.; Lombardo, F.; Dominy, B.W.; Feeney, P.J. Experimental and computational approaches to estimate solubility and permeability in drug discovery and development settings. *Adv. Drug Deliv. Rev.* **2001**, *46*, 3–26. [[CrossRef](#)] [[PubMed](#)]
49. Daina, O.; Michielin, O.; Zoete, V. SwissADME: A free web tool to evaluate pharmacokinetics, druglikeness and medicinal chemistry friendliness of small molecules. *Sci. Rep.* **2017**, *7*, 42717. [[CrossRef](#)]
50. Veber, D.F.; Johnson, S.R.; Cheng, H.Y.; Smith, B.R.; Ward, K.W.; Kopple, K.D. Molecular properties that influence the oral bioavailability of drug candidates. *J. Med. Chem.* **2002**, *45*, 2615–2623. [[CrossRef](#)]

51. Zhou, T.-J.; Sun, L.-G.; Gao, Y.; Goldsmith, E.J. Crystal structure of the MAP3K TAO2 kinase domain bound by an inhibitor Staurosporine. *Acta Biochim. Biophys. Sin.* **2006**, *38*, 385–392. [[CrossRef](#)]
52. Fang, C.-Y.; Lai, T.-C.; Hsiao, M.; Chang, Y.-C. The diverse roles of TAO kinases in health and diseases. *Int. J. Mol. Sci.* **2020**, *21*, 7463. [[CrossRef](#)]
53. Chen, Z.; Cobb, M.H. Regulation of stress-responsive mitogen-activated protein (MAP) kinase pathways by TAO2. *J. Biol. Chem.* **2001**, *276*, 16070–16075. [[CrossRef](#)] [[PubMed](#)]
54. Burton, J.C.; Antoniades, W.; Okalova, J.; Roos, M.M.; Grimsey, N.J. Atypical p38 signaling, activation, and implications for Disease. *Int. J. Mol. Sci.* **2021**, *22*, 4183. [[CrossRef](#)] [[PubMed](#)]
55. Boyd, M.R.; Paull, K.D. Some practical considerations and applications of the national cancer institute in vitro anticancer drug discovery screen. *Drug Dev. Res.* **1995**, *34*, 91–109. [[CrossRef](#)]
56. Mosmann, T. Rapid colorimetric assay for cellular growth and survival: Application to proliferation and cytotoxicity assays. *J. Immunol. Meth.* **1983**, *65*, 55–63. [[CrossRef](#)]
57. Hocquet, A.; Langgård, M. An evaluation of the MM+ force field. *J. Mol. Model.* **1998**, *4*, 94–112. [[CrossRef](#)]
58. Stewart, J.J.P. Optimization of parameters for semiempirical methods I. *Method. J. Comput. Chem.* **1998**, *10*, 209–220. [[CrossRef](#)]
59. Hsu, K.C.; Chen, Y.F.; Lin, S.R.; Yang, J.M. iGEMDOCK: A graphical environment of enhancing GEMDOCK using pharmacological interactions and post-screening analysis. *BMC Bioinform.* **2011**, *12*, S33. [[CrossRef](#)]

Disclaimer/Publisher’s Note: The statements, opinions and data contained in all publications are solely those of the individual author(s) and contributor(s) and not of MDPI and/or the editor(s). MDPI and/or the editor(s) disclaim responsibility for any injury to people or property resulting from any ideas, methods, instructions or products referred to in the content.